Available online at www.sciencedirect.com
ScienceDirect
Journal of Computational Physics 226 (2007) 852–878
JOURNAL OF COMPUTATIONAL PHYSICS
www.elsevier.com/locate/jcp

The incorporation of the semi-implicit linear equations into Newton's method to solve radiation transfer equations

Britton Chang *

Center for Applied Scientific Computing, Lawrence Livermore National Laboratory, P.O. Box 808 L-561, Livermore, CA 94551, United States

Received 14 July 2006; received in revised form 27 April 2007; accepted 3 May 2007
Available online 23 June 2007

Abstract

For large time steps, the nonlinear equations of radiation transfer may not be solved adequately by the semi-implicit linear approximation to yield physical solutions. This deficiency is rectified in three steps: the equations of the semi-implicit linear method are modified, the modified equations are incorporated into Newton's method to solve nonlinear equations, and the transfer equations are solved by the resulting method. The new method also uses the Photon Free Method to search for the solution in a lower dimensional space than the space of the underlying transfer equations. Two algorithms are developed from the new method; they solve the modified semi-implicit linear equations by different approaches. The first is a physics approach; it solves the linear equations approximately by the Grey Transport Approximation. The second is a mathematical approach; it solves the linear equations exactly by the Sherman–Morrison–Woodbury formula of linear algebra. However, both algorithms yield the solution to the nonlinear system derived by the Photon Free Method. Therefore, their solutions are equal to within the specified tolerance of the nonlinear solver. Moreover, both methods can take advantage of the unconditional stability which comes with the implicit differencing of the time derivative. The time step which both methods can take is much larger than the time step in which time discretization error is discernible. We shall relate the mathematical approach to the Photon Free Method. Numerical results for three test problems are presented.

Keywords: Radiation transport; Nonlinear systems, Newton

1. Introduction

For large time steps, the semi-implicit linear approximation (SiL) [20] of the radiation transfer equations, used by conventional deterministic methods [3,20,23,24] to solve the equations of radiation transfer, was found [11] to yield unphysical solutions. This finding was unexpected for two reasons: the time derivatives of the SiL equations are differenced implicitly, and the SiL equations merge into the radiation equations as the time step decreases to zero. Since this abnormal response of the SiL solution to large time steps is absent

* Tel.: +1 925 423 6416; fax: +1 925 423 2993.
E-mail address: bchang@llnl.gov

0021-9991/$ - see front matter
doi:10.1016/j.jcp.2007.05.038

from the solutions [6,21] of the implicitly differenced, multi-group, discrete ordinate, finite difference nonlinear equations of radiative transfer from which the SiL equations are derived, this development compelled us to reassess the SiL approximation in the context of a nonlinear solver. Three questions guided our assessment. Can the shortcomings of the SiL approximation be corrected? Can the corrected equations be used to solve the underlying nonlinear equations? Can the solver, built on top of the corrected equations, be linked to the photon free method (PFM) [11] which optimizes the solution search of Newton's method by seeking the solution in a space of much lower dimensionality than the space of the radiation equations?

The short answer to these questions is the affirmative for all three. Two nonlinear solvers are developed from the modified SiL equations. Both are, however, unconventional applications of Newton's method; the linear system which determines the next iterate in Newton's method is not the Jacobian of the nonlinear system. The difference between the two algorithms is that the linear system is approximated in the first algorithm but is not approximated in the second algorithm. Both methods can be considered to be quasi-Newton methods [18]. These answers are discussed in more detail below.

The assumptions of the SiL method which restrict the time step that it can take accurately are: the coefficients of the equations of radiative transfer can be frozen to their values at the beginning of a time step, and the black body emission function can be linearized about the temperature at the beginning of the time step. Both assumptions can be eliminated from the SiL approximation by minor modifications of its equations. Freezing and linearizing can be considered to be the two lowest order approximations of a nonlinear function by a Taylor series; freezing is the zeroth order and linearizing is the first-order. In our modification of the SiL method, we approximate the nonlinear equations not at the temperature which is at the beginning of a time step as in the SiL method, but at the current temperature which is needed by Newton's iteration. Furthermore, our method linearizes not only the Planckian, but also the coefficients of the nonlinear equations. The goal of our modification is to formulate an equation not for the solution but for the *change* in the solution which is needed to update the solution in Newton's method.

If the radiation equations are solved by Newton's method, then the incorporation of the modified SiL equations as the linear step in Newton's method is straightforward. However the result is not the most efficient method for solving the radiation equations, since the solution to the radiation equations can be obtained from the much smaller but equivalent system of equations derived by the PFM method. In order to take advantage of this reduced system, the modified SiL equations are incorporated into the PFM, as we shall see, in an unconventional way. The result is a hybrid method in which the Jacobian of the PFM is replaced by a transport equation which can be preconditioned by Grey Transport Acceleration [20] and by Diffusion Synthetic Acceleration [2,4,8,9,19,22].

However, when the radiation equations are linearized to the accuracy required by Newton's method, anisotropy is introduced into the pseudo scattering operator of the SiL transport equation. This is an unfortunate development, because the modified equation can not be solved *exactly* by the GTA method [20] which is designed to solve a transport equation with isotropic scattering. In this paper, we shall solve this equation by two different methods. The first method (to be denoted as the INL method), which assumes weak anisotropic scattering, can be described as follows: we set the anisotropic term to zero, then solve the resulting isotropic equation by GTA + DSA preconditioning, and then equate the solution to the isotropic equation to the solution to the anisotropic equation. The second method (to be denoted as the SMW method) solves the transport equation with anisotropic scattering by the Sherman–Morrison–Woodbury (SMW) formula of linear algebra [15]. The algorithm built around the SMW formula, as we shall see, is a generalization of the transport technique to solve a mono-energetic transport equation with isotropic scattering by deriving a 'discrete integral equation' for the 'scalar flux' from the transport equation for the angular flux.

Both nonlinear solvers (INL and SWM) are explained in terms of pseudo-code. The SiNL method, to which the INL method simplifies when the coefficients of the nonlinear system are temperature independent, is developed in order to show the error, caused by the freezing of the coefficients of the radiation equations, in isolation from other errors by producing a solution which differs from the 'exact' solution by only the effect created by the freezing process. The INL, SMW, and SiNL methods are tested on three problems; the results of these tests are presented in Section 6. The nonlinear equations which are solved by these nonlinear methods are described in Section 2. In order to relate these solvers to the solver of the PFM, the PFM is reviewed in Section 3. The incorporation of the SiL approximation into Newton's method is presented in Section 4; it is in

this section where the Jacobian equation of the PFM method is replaced by a transport equation with anisotropic scattering. The isotropicization of this transport equation by the INL method is described in Section 5.1. On the other hand, in Section 5.2, we shall show that the transport equation with anisotropic scattering can be solved exactly by the SMW formula. The numerical results of 3 test problems are presented in Section 6. We summarize the developments of this paper in Section 7. The relationship between the SMW solver and the PFM solver is drawn in Section 7.1. The SiL method is assessed in the context of the INL and SMW methods in Section 7.2.

2. The multi-group and the discrete-ordinate approximation for radiative transfer

For clarity of exposition, we restrict our discussion to slab geometry and local thermodynamic equilibrium. In the absence of scattering, material motion, and heat conduction, the multi-group, discrete-ordinate equations of radiative transfer, Section VII.C of [2], consist of the transport equation:

$$\frac{1}{c}\frac{\partial \psi_{g,d}}{\partial t}+\mu_d\frac{\partial \psi_{g,d}}{\partial x}+\sigma_g(T)\psi_{g,d}=\sigma_g(T)B_g(T)+s_{g,d}\quad \begin{matrix} g=1,\ldots,n_{\hat{g}} \\ d=1,\ldots,n_{\hat{d}} \end{matrix} \tag{2.1}$$

for the intensity $\psi_{g,d}$, and the material equation

$$C_p(T)\frac{\partial T}{\partial t}=\sum_{g=1}^{n_{\hat{g}}}\sum_{d=1}^{n_{\hat{d}}}\sigma_g(T)w_d(\psi_{g,d}-B_g(T))+q \tag{2.2}$$

for the temperature T, where

$$B_g(T)=\int_{\nu_{g-\frac{1}{2}}}^{\nu_{g+\frac{1}{2}}}\frac{4\pi h\nu^3}{c^2}\frac{\mathrm{e}^{-h\nu/kT}}{1-\mathrm{e}^{-h\nu/kT}}\mathrm{d}\nu$$

is the group integrated[1] Planck function,

$$C_p(T)=\rho(T)C_v(T),$$

is the product of the mass density $\rho(T)$ and the heat capacity $C_v(T)$, and $\{w_d\}$ is the set of quadrature weights which sums to 2. In these equations, c is the speed of light, h is Planck's constant, k is Boltzmann's constant, g is the group index, d is the direction index, $\sigma_g(T)$ is the group averaged cross section, $s_{g,d}$ is a frequency and direction dependent external radiation source, and q is an external heat source.

If the system is discretized by the backward Euler Method[2], and if the superscript n represents the beginning of a time step and the absence of a superscript represents the end of a time step, we have

$$\mu_d\frac{\partial \psi_{g,d}}{\partial x}+\left(\sigma_g(T)+\frac{1}{c\Delta t_n}\right)\psi_{g,d}=\sigma_g(T)B_g(T)+s_{g,d}+\frac{\psi^n_{g,d}}{c\Delta t_n},$$

$$C_p(T)\frac{T-T^n}{\Delta t_n}=\sum_{g=1}^{n_{\hat{g}}}\sum_{d=1}^{n_{\hat{d}}}\sigma_g(T)w_d(\psi_{g,d}-B_g(T))+q.$$

The streaming operator can be discretized by many finite element or finite difference techniques, e.g. the Petrov–Galerkin method [16], the Diamond Difference method [10], the Discontinuous Galerkin method [25], the Corner Balance method [1], the Linear Discontinuous method [19], the Weighted Diamond Difference method [7], etc. As a result of the discretization, the spatial derivative can be expressed as a matrix, which we denote as D, and the boundary conditions can be expressed as a source term, which we denote as $b_{g,d}$. Each discretization, however, lays out ψ on a mesh in its own way. For some discretizations, ψ is node centered, for others, ψ is zone centered and face centered, and for a few, ψ is both. For the sake of clarity, let the discretization of the spatial derivative be zone centered. Although such a discretization is highly inaccurate and is highly unlikely to

[1] Normalization of $B_\nu(T)$: $\int_0^\infty \mathrm{d}\nu\int_{-1}^{1}\mathrm{d}\mu\frac{4\pi h\nu^3}{c^2}\frac{\mathrm{e}^{-h\nu/kT}}{1-\mathrm{e}^{-h\nu/kT}}=\frac{8\pi^5k^4T^4}{15h^3c^2}$.

[2] A higher order backward difference formula may be able to take advantage of ability of the PFM and of the new method to take large time steps stably.

be used in a simulation, this choice simplifies our presentation. Assuming that $\psi_{g,d}$, T, the external sources, and the boundary condition $b_{g,d}$ are zone centered arrays, that D is a matrix which operates on zone centered arrays, and that $\sigma_g(T)$ and $C_p(T)$ are diagonal matrices whose entries are nonlinear functions of T, the discrete system of nonlinear equations can be written as

$$(\mu_d D + \sigma_g(T) + (c\Delta t_n)^{-1} I)\psi_{g,d} = \sigma_g(T)B_g(T) + s_{g,d} + (c\Delta t_n)^{-1}\psi^n_{g,d} + b_{g,d},$$
$$C_p(T)\frac{T - T^n}{\Delta t_n} = \sum_{g=1}^{n_{\hat{g}}}\sum_{d=1}^{n_{\hat{d}}}\sigma_g(T)w_d(\psi_{g,d} - B_g(T)) + q.$$

The first equation of the system above can be written more concisely by defining the matrix on the left-hand side (lhs) as

$$H_{g,d}(T) \equiv \mu_d D + \sigma_g(T) + (c\Delta t_n)^{-1} I, \tag{2.3}$$

and the last three terms on the right-hand side (rhs) as $f^n_{g,d} \equiv s_{g,d} + (c\Delta t_n)^{-1}\psi^n_{g,d} + b_{g,d}$ to yield

$$\begin{cases} H_{g,d}(T)\psi_{g,d} = \sigma_g(T)B_g(T) + f^n_{g,d}, \\ C_p(T)\frac{T-T^n}{\Delta t_n} = \sum_{g=1}^{n_{\hat{g}}}\sum_{d=1}^{n_{\hat{d}}}\sigma_g(T)w_d(\psi_{g,d} - B_g(T)) + q. \end{cases} \tag{2.4}$$

To prove the convergence of an algorithm, it is convenient to denote the 'true' solution of (2.4) by $\psi^*_{g,d}$ and T^*; these variables satisfy

$$\begin{cases} H_{g,d}(T^*)\psi^*_{g,d} = \sigma_g(T^*)B_g(T^*) + f^n_{g,d}, \\ C_p(T^*)\frac{T^*-T^n}{\Delta t_n} = \sum_{g=1}^{n_{\hat{g}}}\sum_{d=1}^{n_{\hat{d}}}\sigma_g(T^*)w_d(\psi^*_{g,d} - B_g(T^*)) + q. \end{cases} \tag{2.5}$$

3. A summary of the photon free method

The PFM solves the first equation of (2.4) for $\psi_{g,d}$, since the matrix $H_{g,d}(T)$, which is without scattering, is easy to invert, and then substitute the solution $\psi_{g,d} = H^{-1}_{g,d}(\sigma_g(T)B_g(T) + f^n_{g,d})$ into the second equation of (2.4) to obtain the nonlinear equation,

$$C_p(T)\frac{T - T^n}{\Delta t_n} = \sum_{g,d=1}^{n_{\hat{g}},n_{\hat{d}}}\sigma_g(T)w_d(H^{-1}_{g,d}(\sigma_g(T)B_g(T) + f^n_{g,d}) - B_g(T)) + q, \tag{3.1}$$

which is then solved by Newton's method. The matrix, $H^{-1}_{g,d}$, in (3.1) is known as the sweeping operator in transport theory; its action on the vector $\sigma_g(T)B_g(T)$ is operationally equivalent to a matrix–vector product.

If we can find the T that solves (3.1), then we also have the solution to the underlying system (2.4). The reason is as follows; if we substitute the T that solves (3.1) into the first equation of (2.4), then we can complete the solution of (2.4) by back-solving the first equation of (2.4) for the intensity $\psi_{g,d}$. Let us introduce notation for solving (3.1). If we define, $\mathcal{F}(T)$, as the nonlinear residual of (3.1),

$$\mathcal{F}(T) \equiv q + \sum_{g,d=1}^{n_{\hat{g}},n_{\hat{d}}}\sigma_g(T)w_d(H^{-1}_{g,d}(\sigma_g(T)B_g(T) + f^n_{g,d}) - B_g(T)) - C_p(T)\frac{T - T^n}{\Delta t_n}, \tag{3.2}$$

then (3.1) can be written as

$$\mathcal{F}(T) = 0. \tag{3.3}$$

Nonlinear solvers for (3.3) require the evaluation of $\mathcal{F}(T)$, which is facilitated by the first equation of (2.4). For the iterate, T_k, it is straightforward to evaluate the terms: $C_p(T_k)$, $\sigma_g(T_k)$, and $B_g(T_k)$. However, the evaluation of $H^{-1}_{g,d}(\sigma(T_k)B_g(T_k) + f^n_{g,d})$ is more involved; it is determined by solving the first equation of (2.4) $H_{g,d}(T_k)\psi_{g,d} = \sigma_g(T_k)B_g(T_k) + f^n_{g,d}$.

Let T_k be the current iterate. The goal of an iterative solver is to reduce the nonlinear residual $\mathcal{F}(T)$ with each iteration. Newton's method for solving (3.3) starts with an initial guess, T_0, and finds the new iterate by solving the linear system

$$\mathbf{J}\delta T = -\mathcal{F}(T_k),$$

where

$$\mathbf{J} \equiv \left.\frac{\partial \mathcal{F}(T)}{\partial T}\right|_{T_k}$$

is the Jacobian matrix formed by the partial derivatives of $\mathcal{F}$ evaluated at T_k ($\mathbf{J}$ is given in detail in Appendix). The new iterate is then determined by

$$T_{k+1} = T_k + \delta T.$$

However, $\|\mathcal{F}(T_{k+1})\|$ may be larger than $\|\mathcal{F}(T_k)\|$; the Newton step δT fails to satisfy the goal of the iterative solver. In order to achieve this goal, the step is reduced by a factor of λ, which is less than *1*, in the following way:

$$T_{k+1} = T_k + \lambda\delta T.$$

If this new iterate fails to reduce the 'nonlinear residual' $\mathcal{F}$, then λ is reduced further. This process continues until either an iterate, which decreases the nonlinear residual, is found, or λ is reduced to roundoff which triggers the process to terminate with the declaration that 'Newton's method failed, because $\mathcal{F}(T_k)$, which in not 0, is not reduced by δT'.

Let us introduce into (2.4) notation for the temperature dependent functions, matrices, temperature derivatives of these functions, and temperature derivatives of these matrices at the temperature at which they are evaluated; the superscript k represent their values at the temperature T_k, e.g.

$$C_p^k \equiv C_p(T_k), \quad \dot{C}_p^k \equiv \left.\frac{\partial C_p}{\partial T}\right|_{T_k},$$

$$\sigma_g^k \equiv \sigma_g(T_k), \quad \dot{\sigma}_g^k \equiv \left.\frac{\partial \sigma_g}{\partial T}\right|_{T_k},$$

$$B_g^k \equiv B_g(T_k), \quad \dot{B}_g^k \equiv \left.\frac{\partial B_g}{\partial T}\right|_{T_k},$$

$$H_{g,d}^k \equiv H_{g,d}(T_k), \quad \dot{H}_{g,d}^k \equiv \dot{\sigma}_g^k.$$

The PFM algorithm, derived in [11], for solving (2.4) is

Algorithm 1 (The photon free method)

$T_0 = T^n$
for $k = 0, 1, \ldots$
1. $H_{g,d}^k \psi_{g,d} = \sigma_g^k B_g^k + f_{g,d}^n$
2. $\mathcal{F}(T_k) = q - C_p^k \frac{T_k - T^n}{\Delta t_n} + \sum_{g=1}^{n_g}\sum_{d=1}^{n_d} \sigma_g^k w_d(\psi_{g,d} - B_g^k)$
3. if $\|\mathcal{F}(T_k)\| > \text{tol}$
4. $\quad \mathbf{J}\delta T = -\mathcal{F}(T_k)$
5. $\quad \lambda = 1$
6. $\quad T_\lambda = T_k + \lambda\delta T$
7. $\quad$ if $\|\mathcal{F}(T_\lambda)\| > \|\mathcal{F}(T_k)\|$
8. $\quad\quad \lambda = \lambda/2$, go to 6
9. $\quad$ else
10. $\quad\quad T_{k+1} = T_\lambda$
11. $\quad$ end if
12. else

13. break (solution found)
14. end if

end for.

The procedure, which is between line 6 and line 11 in the above pseudo code, is the simplest example[3] of a line search algorithm; our code uses the Armijo line search algorithm [5].

Remark 1. If **J** is nonsingular, then Algorithm 1 converges to the solution of (2.4) when $\mathcal{F}(T_k) = 0$.

Proof. Since **J** is nonsingular, Algorithm 1 can proceed. If $\mathcal{F}(T_k) = 0$, then by line 2 of Algorithm 1, we have

$$C_p^k \frac{T_k - T^n}{\Delta t_n} = \sum_{g=1}^{n_{\hat{g}}} \sum_{d=1}^{n_{\hat{d}}} \sigma_g^k w_d (\psi_{g,d} - B_g^k) + q, \tag{3.4}$$

where $\psi_{g,d}$ is determined by line 1 of Algorithm 1.

$$H_{g,d}^k \psi_{g,d} = \sigma_g^k B_g^k + f_{g,d}^n. \tag{3.5}$$

Comparing the pair, (3.4) and (3.5), to the pair in (2.5), we have $\psi_{g,d} = \psi_{g,d}^*$ and $T_k = T^*$. □

Since the cost of Newton's method for solving a nonlinear system increases with the size of the system, the PFM method achieves efficiency by solving an equivalent but much smaller system than the underlying system of radiation equations.

4. Derivation of the modified SiL approximation

The goal of this section is to solve the PFM system of Eq. (3.3) by a modified SiL algorithm. Our modification of the SiL algorithm is developed in two stages. An algorithm for solving the radiative transfer equations with *lagged* coefficients is introduced in the first stage in order to underscore the terms which are inserted into the SiL equations by our modification even when the heat capacity and the cross section are temperature independent. To lag a coefficient is to treat the coefficient as if it were temperature independent within a time step, and to fix the value of the coefficient to its value at the beginning of the time step. Then, in the second stage, the temperature effects of a temperature dependent heat capacity and a temperature dependent cross section are incorporated into the modified algorithm.

The modified equations are derived by approximating the system of nonlinear functions (2.4) by a first-order Taylor series. To facilitate the approximating process, we introduce the $[\cdot]$ notation to denote the operator which converts a vector of length $n_{\hat{x}}$ into a diagonal matrix of order $n_{\hat{x}}$ by inserting the entries of the vector into the diagonal entries of the matrix,

$$[x] \in R^{n_{\hat{x}} \times n_{\hat{x}}} \equiv \mathrm{diag}(x) \quad \text{for } x \in R^{n_{\hat{x}} \times 1}.$$

We also need the formula, $[x]y = [y]x$, to manipulate these diagonal matrices.

Remark 2. If x and y are vectors of length $n_{\hat{x}}$, then $[x]y = [y]x$.

Proof. For each i, $1 \leqslant i \leqslant n_{\hat{x}}$, component i of the vector $[x]y$ is

$$([x]y)_i = x_i y_i = y_i x_i = ([y]x)_i \quad \square$$

[3] The factor of 2 in line 8 is arbitrary. A more efficient algorithm selects a reduction factor that depends on the rejected nonlinear residuals. We remind the reader that the calculation of $\mathcal{F}(T_\lambda)$ on line 7 requires the solution of the transport equation at the current iterate T_λ, $H_{g,d}(T_\lambda)\psi_{g,d} = \sigma_g(T_\lambda)B_g(T_\lambda) + f_{g,d}^n$.

4.1. Modifications with lagged coefficients

In this paper, a matrix, which is either temperature independent or lagged, is superscript-less. In this subsection, let $H_{g,d}$, σ_g, and C_p denote the lagged approximations of $H_{g,d}(T)$, $\sigma_g(T)$, and $C_p(T)$, respectively.

The derivation of the SiL approximation of (2.4) begins by lagging $H_{g,d}(T)$, $\sigma_g(T)$, and $C_p(T)$ to yield

$$\begin{cases} H_{g,d}\psi^{lag}_{g,d} = \sigma_g B_g(T) + f^n_{g,d}, \\ C_p \frac{T-T^n}{\Delta t_n} = \sum_{g=1}^{n_{\hat{g}}} \sum_{d=1}^{n_{\hat{d}}} \sigma_g w_d (\psi^{lag}_{g,d} - B_g(T)) + q. \end{cases} \tag{4.1}$$

The SiL approximation then expands $B_g(T)$ about the temperature at the beginning of the time step T^n. However, in our modification of the SiL equations, we expand both $B_g(T)$ and $(T - T^n)$ linearly about the *current* iterate T_k:

$$B_g(T) \approx B^k_g + [\dot{B}^k_g](T - T_k), \quad \text{and} \quad T - T^n = (T_k - T^n) + (T - T_k).$$

Substituting these expansions into (4.1) yields our modification of the SiL approximation

$$\begin{aligned} &H_{g,d}\psi^{\mathrm{SiL}}_{g,d} = \sigma_g(B^k_g + [\dot{B}^k_g](T - T_k)) + f^n_{g,d}, \\ &\frac{C_p}{\Delta t_n}(T - T_k) = \sum_{g=1}^{n_{\hat{g}}} \sum_{d=1}^{n_{\hat{d}}} \sigma_g w_d (\psi^{\mathrm{SiL}}_{g,d} - B^k_g - [\dot{B}^k_g](T - T_k)) + q - \frac{C_p}{\Delta t_n}(T_k - T^n). \end{aligned} \tag{4.2}$$

Larsen's SiL approximation [20] can be obtained from (4.2) by dropping the last term, $C_p \cdot (T_k - T^n)/\Delta t_n$, on the rhs of the second equation of (4.2), and by evaluating both the Planckian and the Planckian's temperature derivative at T^n. The linear system (4.2) can be solved by Larsen's method [20]; the second equation of (4.2) is solved for $T - T_k$ and the result is substituted into the first equation of (4.2) to yield

$$H_{g,d}\psi^{\mathrm{SiL}}_{g,d} = \hat{\alpha}^k_g \left(\sum_{g'=1}^{n_{\hat{g}}} \sum_{d'=1}^{n_{\hat{d}}} \sigma_{g'} w_{d'} (\psi^{\mathrm{SiL}}_{g',d'} - B^k_{g'}) + q - C_p \frac{T_k - T^n}{\Delta t_n} \right) + \sigma_g B^k_g + f^n_{g,d}, \tag{4.3}$$

where[4]

$$\hat{\alpha}^k_g \equiv \frac{\sigma_g [\dot{B}^k_g]}{\frac{C_p}{\Delta t_n} + \sum_{g=1,d=1}^{n_{\hat{g}},n_{\hat{d}}} \sigma_g w_d [\dot{B}^k_g]}. \tag{4.4}$$

The operator $\hat{\alpha}^k_g C_p (T_k - T^n)/\Delta t_n$, which is the last term within the parenthesis on the rhs of (4.3), is absent in Larsen's equation (2.23) of [20]. After (4.3) is solved for $\psi^{\mathrm{SiL}}_{g,d}$, Larsen completes the solution to (4.2) by substituting $\psi^{\mathrm{SiL}}_{g,d}$ into the second equation of (4.2) to obtain T. Thus, Larsen's method can be interpreted as an algorithm to determine T.

In fact, we shall use Larsen's method to determine a new temperature iterate in Newton's method to solve (4.1). In order to do so, we need notation. Let T_k denote the temperature, and $\psi^{k,\mathrm{lag}}_{g,d}$ denote the intensity at the kth stage of Newton's iteration. The procedure to determine the new iterate T_{k+1} by Larsen's method is derived in three steps. The first step is to define $\psi^{\mathrm{SiL}}_{g,d}$ as

$$\psi^{\mathrm{SiL}}_{g,d} \equiv \psi^{k,\mathrm{lag}}_{g,d} + \delta\psi^k_{g,d}, \tag{4.5}$$

where $\psi^{k,\mathrm{lag}}_{g,d}$ is determined by the first equation of (4.1) with the temperature in that equation set to T_k

$$H_{g,d}\psi^{k,\mathrm{lag}}_{g,d} \equiv \sigma_g B^k_g + f^n_{g,d}. \tag{4.6}$$

The second step is to derive an equation to determine $\delta\psi^k_{g,d}$. This equation can be obtained by substituting (4.5) into (4.3). Using (4.6) to simplify the result of the substitution yields

[4] For a nonsingular diagonal A, such as the matrix in the 'denominator' of (4.4), we denote the inverse of A as $\frac{I}{A}$, and denote the solution to $Ax = b$ as $\frac{b}{A}$ to emphasize the diagonality of A.

$$H_{g,d}\delta\psi^k_{g,d} - \hat{\alpha}^k_g \sum_{g'=1}^{n_{\hat{g}}} \sum_{d'=1}^{n_{\hat{d}}} \sigma_{g'} w_{d'} \delta\psi^k_{g',d'} = \hat{\alpha}^k_g \mathcal{F}_{\text{lag}}(T_k), \tag{4.7}$$

where

$$\mathcal{F}_{\text{lag}}(T_k) = q + \sum_{g=1}^{n_{\hat{g}}} \sum_{d=1}^{n_{\hat{d}}} \sigma_g w_d (\psi^{k,\text{lag}}_{g,d} - B^k_g) - C_p \frac{T_k - T^n}{\Delta t_n} \tag{4.8}$$

is the PFM nonlinear residual for the pair in (4.1) at temperature T_k. The third step is to substitute (4.5) into the second equation of (4.2) and then use (4.8) to collect terms to yield

$$T = T_k + \frac{\mathcal{F}_{\text{lag}}(T_k) + \sum_{g=1}^{n_{\hat{g}}} \sum_{d=1}^{n_{\hat{d}}} \sigma_g w_d \delta\psi^k_{g,d}}{C_p/\Delta t_n + \sum_{g=1}^{n_{\hat{g}}} \sum_{d=1}^{n_{\hat{d}}} \sigma_g w_d [\dot{B}^k_g]}. \tag{4.9}$$

The collection of Eqs. (4.6), (4.8), (4.7), and (4.9), can be crafted into an algorithm to solve (4.1).

Algorithm 2 (Semi-implicit nonlinear method for lagged coefficients)

$T_0 = T^n$
for $k = 0, 1, \ldots$
1. $H_{g,d}\psi^{k,\text{lag}}_{g,d} = \sigma_g B^k_g + f^n_{g,d}$
2. $\mathcal{F}_{\text{lag}}(T_k) = q - C_p \frac{T_k - T^n}{\Delta t_n} + \sum_{g=1}^{n_{\hat{g}}} \sum_{d=1}^{n_{\hat{d}}} \sigma_g w_d (\psi^{k,\text{lag}}_{g,d} - B^k_g)$
3. if $\|\mathcal{F}_{\text{lag}}(T_k)\| > \text{tol}$
4. $\quad H_{g,d}\delta\psi^k_{g,d} - \hat{\alpha}^k_g \sum_{g'=1}^{n_{\hat{g}}} \sum_{d'=1}^{n_{\hat{d}}} \sigma_{g'} w_{d'} \delta\psi^k_{g',d'} = \hat{\alpha}^k_g \mathcal{F}_{\text{lag}}(T_k)$
5. $\quad \lambda = 1$
6. $\quad T_\lambda = T_k + \lambda \frac{\mathcal{F}_{\text{lag}}(T_k) + \sum_{g=1}^{n_{\hat{g}}} \sum_{d=1}^{n_{\hat{d}}} \sigma_g w_d \delta\psi^k_{g,d}}{C_p/\Delta t_n + \sum_{g=1}^{n_{\hat{g}}} \sum_{d=1}^{n_{\hat{d}}} \sigma_g w_d [\dot{B}^k_g]}$
7. $\quad$ if $\|\mathcal{F}_{\text{lag}}(T_\lambda)\| > \|\mathcal{F}_{\text{lag}}(T_k)\|$
8. $\quad\quad \lambda = \lambda/2$, go to 6
9. $\quad$ else
10. $\quad\quad T_{k+1} = T_\lambda$
11. $\quad$ end if
12. else
13. $\quad$ break, (solution found)
14. end if

end for.

Remark 3. Assume that line searching is 'turned off' in Algorithm 2, the zeroth iterate of Algorithm 2 is the SiL solution of [20].

Proof. If, in Algorithm 2, we fix λ to 1 and we set $k = 0$, then the lines 1, 2, 4, 6, and 10 for this iterate are:

$$H_{g,d}\psi^{k,\text{lag}}_{g,d} = \sigma_g B^k_g + f^n_{g,d}, \tag{4.10}$$

$$\mathcal{F}_{\text{lag}}(T_k) = q - C_p \frac{T_k - T^n}{\Delta t_n} + \sum_{g=1}^{n_{\hat{g}}} \sum_{d=1}^{n_{\hat{d}}} \sigma_g w_d (\psi^{k,\text{lag}}_{g,d} - B^k_g), \tag{4.11}$$

$$H_{g,d}\delta\psi^k_{g,d} - \hat{\alpha}^k_g \sum_{g'=1}^{n_{\hat{g}}} \sum_{d'=1}^{n_{\hat{d}}} \sigma_{g'} w_{d'} \delta\psi^k_{g',d'} = \hat{\alpha}^k_g \mathcal{F}_{\text{lag}}(T_k), \tag{4.12}$$

and

$$T_{k+1} = T_k + \frac{\mathcal{F}_{\text{lag}}(T_k) + \sum_{g=1}^{n_{\hat{g}}} \sum_{d=1}^{n_{\hat{d}}} \sigma_g w_d \delta\psi^k_{g,d}}{C_p/\Delta t_n + \sum_{g=1}^{n_{\hat{g}}} \sum_{d=1}^{n_{\hat{d}}} \sigma_g w_d [\dot{B}^k_g]}. \tag{4.13}$$

If we substitute (4.11) into (4.12) and (4.13), add (4.10) and (4.12), and apply (4.5) to the result, we have

$$H_{g,d}\psi^{\mathrm{SiL}}_{g,d} = \hat{\alpha}^k_g\left(\sum_{g'=1}^{n_{\hat{g}}}\sum_{d'=1}^{n_{\hat{d}}}\sigma_{g'}w_{d'}(\psi^{\mathrm{SiL}}_{g',d'} - B^k_{g'}) + q - C_p\frac{T_k - T^n}{\Delta t_n}\right) + \sigma_g B^k_g + f^n_{g,d},$$

$$T_{k+1} = T_k + \frac{\left(\sum_{g=1}^{n_{\hat{g}}}\sum_{d=1}^{n_{\hat{d}}}\sigma_g w_d(\psi^{\mathrm{SiL}}_{g,d} - B^k_g)\right) + q - C_p\frac{T_k - T^n}{\Delta t_n}}{C_p/\Delta t_n + \sum_{g=1}^{n_{\hat{g}}}\sum_{d=1}^{n_{\hat{d}}}\sigma_g w_d[\dot{B}^k_g]}.$$

For $k = 0$, $T_0 = T^n$. Comparing the above pair of equations to Eq. (4.3) and the second equation of (4.2), we have the SiL equation given by (2.23) of [20]. □

Remark 4. If the matrix on the lhs of line 4 of Algorithm 2 is nonsingular, then Algorithm 2 converges to the solution of (4.1) when $\mathcal{F}_{\mathrm{lag}}(T_k) = 0$.

Proof. Since matrix on the lhs of line 4 of Algorithm 2 is nonsingular, then Algorithm 2 can proceed. When $\mathcal{F}_{\mathrm{lag}}(T_k) = 0$, we have the solution to (4.1) for the reasons given in Remark 1. □

In this section in which the heat capacity and the cross section are temperature independent, the SiL equations are modified in a way in which the equations on lines 4 and 6 of the PFM method of Algorithm 1 can be exchanged for the equations on lines 4 and 6 of Algorithm 2. The equations on lines 4 and 6 of both algorithms generate the trial temperature T_λ which goes into line search. If the coefficients of these equations are temperature independent, then Algorithm 2 yields the solution to the PFM system of nonlinear equations (3.3).

4.2. Implicit nonlinear transport method with unfrozen coefficients

In order to incorporate a temperature dependent heat capacity and a temperature dependent cross section into the framework of Algorithm 2 of Section 4.1, the temperature dependent terms of (2.4), $C_p(T)(T - T^n)$, $\sigma_g(T)B_g(T)$, and $\sigma_g(T)\psi_{g,d}$, are linearized about the current temperature T_k.

It is straightforward to expand $C_p(T)(T - T^n)$ and $\sigma_g(T)B_g(T)$. The expansion of $C_p(T)(T - T^n)$ about T_k is

$$C_p(T)(T - T^n) \approx C^k_p(T_k - T^n) + (C^k_p + \dot{C}^k_p[T_k - T^n])(T - T_k), \tag{4.14}$$

and the expansion of $\sigma_g(T)B_g(T)$ about T_k is

$$\sigma_g(T)B_g(T) \approx \sigma^k_g B^k_g + \left(\sigma^k_g[\dot{B}^k_g] + \dot{\sigma}^k_g[B^k_g]\right)(T - T_k). \tag{4.15}$$

However, the expansion of $\sigma_g(T)\psi_{g,d}$ about T_k is complicated. Although the expansion of $\sigma_g(T)$ is straightforward

$$\sigma_g(T) \approx \sigma^k_g + \dot{\sigma}^k_g[T - T_k], \tag{4.16}$$

the expansion of $\psi_{g,d}$, which does not depend explicitly on T, about T_k requires a reference intensity at T_k by which to expand $\psi_{g,d}$. Let $\psi^k_{g,d}$ be that reference intensity which is determined by the first equation of (2.4) with the temperature in that equation set to T_k

$$H^k_{g,d}\psi^k_{g,d} = \sigma^k_g B^k_g + f^n_{g,d}. \tag{4.17}$$

This equation is a generalization of (4.6); the coefficients of (4.17) are evaluated at T_k whereas the coefficients of (4.6) are independent of temperature. Since $\psi_{g,d}$ is the intensity which is determined by the first equation of (2.4) with the temperature in that equation set to T, then we define $\delta\psi^k_{g,d}$ to be the change in the intensity when the temperature in the first equation of (2.4) is changed from T_k to T. These three intensities are related by

$$\psi_{g,d} \equiv \psi^k_{g,d} + \delta\psi^k_{g,d}. \tag{4.18}$$

Therefore, the expansion of $\sigma_g(T)\psi_{g,d}$ about T_k can be determined from the product of (4.16) and (4.18)

$$\begin{aligned}\sigma_g(T)\psi_{g,d} &\approx (\sigma_g^k + \dot{\sigma}_g^k[T-T_k])(\psi_{g,d}^k + \delta\psi_{g,d}^k) \approx \sigma_g^k(\psi_{g,d}^k + \delta\psi_{g,d}^k) + \dot{\sigma}_g^k[T-T_k]\psi_{g,d}^k \\ &= \sigma_g^k(\psi_{g,d}^k + \delta\psi_{g,d}^k) + \dot{\sigma}_g^k[\psi_{g,d}^k](T-T_k),\end{aligned} \tag{4.19}$$

where the second-order term $[T-T_k]\delta\psi_{g,d}^k$ is dropped and $[\psi_{g,d}^k](T-T_k)$ is obtained from $[T-T_k]\psi_{g,d}^k$ by the formula of Remark 2.

Since $H_{g,d}(T)$, defined in (2.3), is the sum of $\sigma_g(T)$ and the temperature independent matrix D, then $\dot{H}_{g,d}^k = \dot{\sigma}_g^k$. Therefore the first-order expansion of $H_{g,d}(T)\psi_{g,d}$ is

$$H_{g,d}(T)\psi_{g,d} \approx H_{g,d}^k(\psi_{g,d}^k + \delta\psi_{g,d}^k) + \dot{\sigma}_g^k[\psi_{g,d}^k](T-T_k). \tag{4.20}$$

The substitution of (4.15) and (4.20) into the first equation of (2.4) and the application of (4.17) to simplify the result yield

$$H_{g,d}^k\delta\psi_{g,d}^k + \dot{\sigma}_g^k[\psi_{g,d}^k](T-T_k) = (\sigma_g^k[\dot{B}_g^k] + \dot{\sigma}_g^k[B_g^k])(T-T_k). \tag{4.21}$$

Substituting (4.14), (4.15) and (4.19) into the second equation of (2.4), collecting terms with (3.2), and rearranging the result slightly, we have

$$\begin{aligned}&\left(\frac{C_p^k + \dot{C}_p^k[T_k - T^n]}{\Delta t_n} + \sum_{g=1}^{n_{\hat{g}}}\sum_{d=1}^{n_{\hat{d}}} w_d(\sigma_g^k[\dot{B}_g^k] + \dot{\sigma}_g^k[B_g^k] - \dot{\sigma}_g^k[\psi_{g,d}^k])\right)(T-T_k) \\ &\quad = \mathcal{F}(T) + \sum_{g=1}^{n_{\hat{g}}}\sum_{d=1}^{n_{\hat{d}}}\sigma_g^k w_d\delta\psi_{g,d}^k.\end{aligned} \tag{4.22}$$

If the diagonal matrix on the lhs of (4.22) is nonsingular,

$$\left(\frac{C_p^k + \dot{C}_p^k[T_k - T^n]}{\Delta t_n} + \sum_{g=1}^{n_{\hat{g}}}\sum_{d=1}^{n_{\hat{d}}} w_d(\sigma_g^k[\dot{B}_g^k] + \dot{\sigma}_g^k[B_g^k] - \dot{\sigma}_g^k[\psi_{g,d}^k])\right)_{i,i} \neq 0, 1 \leqslant i \leqslant n_{\hat{x}}, \tag{4.23}$$

we can solve (4.22) for $(T-T_k)$ and substitute the result into (4.21) to give the transport equation which is driven by pseudo *anisotropic*[5] scattering and by a pseudo external *anisotropic* source

$$H_{g,d}^k\delta\psi_{g,d}^k - \alpha_{g,d}^k\sum_{g'=1}^{n_{\hat{g}}}\sum_{d'=1}^{n_{\hat{d}}}\sigma_g^k w_{d'}\delta\psi_{g',d'}^k = \alpha_{g,d}^k\mathcal{F}(T_k), \tag{4.24}$$

where

$$\alpha_{g,d}^k \equiv \frac{\sigma_g^k[\dot{B}_g^k] + \dot{\sigma}_g^k[B_g^k] - \dot{\sigma}_g^k[\psi_{g,d}^k]}{\frac{C_p^k + \dot{C}_p^k[T_k - T^n]}{\Delta t_n} + \sum_{g=1}^{n_{\hat{g}}}\sum_{d=1}^{n_{\hat{d}}} w_d(\sigma_g^k[\dot{B}_g^k] + \dot{\sigma}_g^k[B_g^k] - \dot{\sigma}_g^k[\psi_{g,d}^k])}. \tag{4.25}$$

Remark 5. The pair (4.21) and (4.22) is a special linear system in which the elimination of either $(T-T_k)$ or $\delta\psi_{g,d}^k$ is easy. The elimination of $(T-T_k)$ from the pair, which requires the assumption (4.23), yields (4.24). On the other hand, the elimination of $\delta\psi_{g,d}^k$ from the pair, which requires the sweeping operator $H_{g,d}^{k,-1}$ to exist, yields

$$\left(\frac{C_p^k + \dot{C}_p^k[T_k - T^n]}{\Delta t_n} + \sum_{g=1}^{n_{\hat{g}}}\sum_{d=1}^{n_{\hat{d}}} w_d(I - \sigma_g^k H_{g,d}^{k,-1})(\sigma_g^k[\dot{B}_g^k] + \dot{\sigma}_g^k[B_g^k] - \dot{\sigma}_g^k[\psi_{g,d}^k])\right)(T-T_k) = \mathcal{F}(T_k), \tag{4.26}$$

which is the equation on line 4 of Algorithm 1 by which the PFM method updates the temperature. The proof of this statement is : the matrix on the lhs of (4.26) is the negative of the **J** given by (8.3). Since the elimination

[5] An anisotropic operator or an anisotropic source means that the operator or the source depends on the direction index d.

of either $(T - T_k)$ or $\delta\psi^k_{g,d}$ from the pair (4.21) and (4.22) improves the efficiency for solving them without altering the solution, then the solutions to the pair obtained by Algorithms 1 and 3 are equal.

The collection of Eqs. (3.2), (4.17), (4.22), (4.24) and (4.25), can be crafted into an algorithm to solve (2.4) with *unlagged* coefficients.

Algorithm 3 (The modified SiL algorithm with unfrozen coefficients).

$T_0 = T^n$
for $k = 0, 1, \ldots$
1. $H^k_{g,d}\psi^k_{g,d} = \sigma^k_g B^k_g + f^n_{g,d}$
2. $\mathcal{F}(T_k) = q - C^k_p \frac{T_k - T^n}{\Delta t_n} + \sum_{g=1}^{n_{\hat{g}}}\sum_{d=1}^{n_{\hat{d}}}\sigma^k_g w_d(\psi^k_{g,d} - B^k_g)$
3. if $\|\mathcal{F}(T_k)\| > \text{tol}$
4. $\quad H^k_{g,d}\delta\psi^k_{g,d} - \alpha^k_{g,d}\sum_{g'=1}^{n_{\hat{g}}}\sum_{d'=1}^{n_{\hat{d}}}\sigma^k_{g'}w_{d'}\delta\psi^k_{g',d'} = \alpha^k_{g,d}\mathcal{F}(T_k)$
5. $\quad \lambda = 1$
6. $\quad T_\lambda = T_k + \lambda \frac{\mathcal{F}(T_k) + \sum_{g=1}^{n_{\hat{g}}}\sum_{d=1}^{n_{\hat{d}}}\sigma_g w_d \delta\psi^k_{g,d}}{\frac{C^k_p + \dot{C}^k_p[T_k - T^n]}{\Delta t_n} + \sum_{g=1}^{n_{\hat{g}}}\sum_{d=1}^{n_{\hat{d}}} w_d(\sigma^k_g[\dot{B}^k_g] + \dot{\sigma}^k_g[B^k_g] - \dot{\sigma}^k_g[\psi^k_{g,d}])}$
7. $\quad$ if $\|\mathcal{F}(T_\lambda)\| > \|\mathcal{F}(T_k)\|$
8. $\quad\quad \lambda = \lambda/2$, go to 6
9. $\quad$ else
10. $\quad\quad T_{k+1} = T_\lambda$
11. $\quad$ end if
12. else
13. $\quad$ break, (solution found)
14. end if

end for.

Remark 6. If, in Algorithm 3, the equation on line 4 is solvable, and the 'denominator' on the rhs of line 6 is nonsingular, then Algorithm 3 converges to the solution of (2.4) when $\mathcal{F}(T_k) = 0$.

Proof. These two assumption enable Algorithm 3 to proceed. When $\mathcal{F}(T_k) = 0$, we have the solution to (2.4) for the reasons given in Remark 1. □

Algorithm 3 generalizes Algorithm 2 by incorporating the temperature derivatives of $C_p(T)$ and $\sigma_g(T)$ into the coupling strength $\alpha^k_{g,d}$ and into the denominator on the rhs of line 6. However, these terms may cause Algorithm 3 to fail by preventing (4.23) to be met.

5. Methods to solve the transport equation of Algorithm 3

The transport equation on the fourth line of Algorithm 3 is a generalization of the transport equation of the SiL approximation which the GTA method is designed to solve. However, the GTA method requires two conditions which may not be met when the coefficients of this equation are temperature dependent. The first condition requires the scattering term to be isotropic; the coupling strength $\alpha^k_{g,d}$ on the lhs of the equation must be independent of the direction index d which occurs when $\dot{\sigma}^k_g = 0$ (see (4.25)). The second condition requires $\alpha^k_{g,d}$ to be positive in order for it to be interpreted as a scattering probability; this condition is met when both $\dot{C}^k_p$ and $\dot{\sigma}^k_g$ are zero.

We shall solve this transport equation with anisotropic scattering by two methods. The first method consists of two steps. In the first step, the coefficient $\alpha^k_{g,d}$ on the lhs of the equation is 'isotropicized' by setting the $\dot{\sigma}^k_g$ term in $\alpha^k_{g,d}$ to zero. In the second step, the solution of 'isotropicized' transport equation is equated to the solution of anisotropic transport equation. The second method solves the transport equation with anisotropic scattering by the Sherman–Morrison–Woodbury (SMW) formula of linear algebra [15].

5.1. Isotropicization of the transport equation

Let

$$\zeta(\varrho(T)) \equiv \left| \frac{T}{\varrho(T)} \frac{\partial \varrho(T)}{\partial T} \right| \tag{5.1}$$

denote the 'sensitivity coefficient' of $\varrho(T)$. The coefficient $\varrho(T)$ is said to be temperature sensitive if $\zeta(\varrho(T)) > 1$, and temperature insensitive if $\zeta(\varrho(T)) < 1$. The INL approximation assumes that $\zeta(\sigma_g^k) < 1$; thus setting $\dot{\sigma}_g^k$ to zero in (4.25) yields

$$\alpha_{g,d}^k \to \tilde{\alpha}_g^k \equiv \frac{\sigma_g^k[\dot{B}_g^k]}{\frac{C_p^k + \dot{C}_p^k[T_k - T^n]}{\Delta t_n} + \sum_{g=1}^{n_{\tilde{g}}} \sum_{d=1}^{n_{\tilde{d}}} w_d \sigma_g^k[\dot{B}_g^k]}. \tag{5.2}$$

Substituting (5.2) into the lhs of the transport equation on line 4 of Algorithm 3 makes the transport equation isotropic and amenable to the GTA method. Although $\tilde{\alpha}_g^k$ of (5.2) and $\hat{\alpha}_g^k$ of (4.4) are similar in form, they are different in content. The coefficient $\tilde{\alpha}_g^k$ of (5.2) is determined by the heat capacity and the cross sections which are evaluated at the *current* temperature T_k. On the other hand, $\hat{\alpha}_g^k$ of (4.4) is determined by the heat capacity and the cross sections which are evaluated at T^n the temperature at the beginning of the time step.

5.2. Solving the transport equation of Algorithm 3 by the Sherman–Morrison–Woodbury formula

Since the GTA method, which is designed to solve a transport equation with isotropic scattering, is unable to 'exactly' solve a transport equation with anisotropic scattering which occurs when the cross section is temperature sensitive, then the goal of this section is to develop a low cost method to solve the transport equation when this situation occurs. Furthermore, the matrix operations on the sixth line of the algorithm are costly. If these matrix operations can be eliminated from the new method, then the efficiency of the new method is further improved. We shall see that the computational costs of the fourth and sixth lines can both be lowered by reducing the number of equations and the number of unknowns in these two lines by the application of the SMW formula [15].

The system of equations on the fourth line can be transformed into a smaller system in four steps: left multiply the fourth line by $w_d H_{g,d}^{k,-1}$, sum the product with respect to d, left multiply the resulting sum by σ_g^k, and sum that product with respect to g. The result is

$$\widetilde{\Phi}^k - \left(\sum_{g=1}^{n_{\tilde{g}}} \sigma_g^k \left(\sum_{d=1}^{n_{\tilde{d}}} w_d H_{g,d}^{k,-1} \alpha_{g,d}^k \right) \right) \widetilde{\Phi}^k = \left(\sum_{g=1}^{n_{\tilde{g}}} \sigma_g^k \left(\sum_{d=1}^{n_{\tilde{d}}} w_d H_{g,d}^{k,-1} \alpha_{g,d}^k \right) \right) \mathcal{F}(T_k), \tag{5.3}$$

where

$$\widetilde{\Phi}^k \equiv \sum_{g=1}^{n_{\tilde{g}}} \sum_{d=1}^{n_{\tilde{d}}} \sigma_g^k w_d \delta\psi_{g,d}^k \in R^{n_{\tilde{x}} \times 1} \tag{5.4}$$

is denoted as F, the 'integrated intensity', in the GTA method [19]. When the $n_{\tilde{x}} \times n_{\tilde{x}}$ 'lambda' matrix,

$$\Lambda^k \equiv \sum_{g=1}^{n_{\tilde{g}}} \sigma_g^k \left(\sum_{d=1}^{n_{\tilde{d}}} w_d H_{g,d}^{k,-1} \alpha_{g,d}^k \right) \in R^{n_{\tilde{x}} \times n_{\tilde{x}}}, \tag{5.5}$$

is substituted into (5.3), we have

$$\widetilde{\Phi}^k - \Lambda^k \widetilde{\Phi}^k = \Lambda^k \mathcal{F}(T_k), \tag{5.6}$$

which is the reduced system of the SMW decomposition[6] of the equation on line 4 of Algorithm 3.

[6] The SMW decomposition of $H_{g,d}^k \delta\psi_{g,d}^k - \alpha_{g,d}^k \sum_{g'=1}^{n_{\tilde{g}}} \sum_{d'=1}^{n_{\tilde{d}}} \sigma_{g'}^k w_{d'} \delta\psi_{g',d'}^k = \alpha_{g,d}^k \mathcal{F}(T_k)$ consists of the pair of equations: (5.6), and $H_{g,d}^k \delta\psi_{g,d}^k = \alpha_{g,d}^k \widetilde{\Phi}^k + \alpha_{g,d}^k \mathcal{F}(T_k)$. The second of the pair is obtained by the substitution of (5.4) into the second term on the lhs of the first equation of the previous sentence. Since, as we shall see, the sixth line of Algorithm 3 needs $\widetilde{\Phi}^k$ but not $\delta\psi_{g,d}^k$, then the second equation of the SMW pair can be omitted from our modification of Algorithm 3.
Eq. (5.6) is also called the Lambda equation of the Lambda Method for solving Line Radiation Transport Equations [17].

Let us turn off 'line search' in Algorithm 3 and direct our thoughts to the equation on the sixth line of the algorithm. On the rhs of the equation, we set $\lambda = 1$ and substitute (5.4) into the 'numerator' to yield

$$T_{k+1} = T_k + \frac{\mathcal{F}(T_k) + \widetilde{\Phi}^k}{\frac{C_p^k + \dot{C}_p^k[T_k - T^n]}{\Delta t_n} + \sum_{g=1}^{n_{\hat{g}}} \sum_{d=1}^{n_{\hat{d}}} w_d \left(\sigma_g^k [\dot{B}_g^k] + \dot{\sigma}_g^k [B_g^k] - \dot{\sigma}_g^k [\psi_{g,d}^k] \right)}. \tag{5.7}$$

At this point, the fourth and the sixth lines of Algorithm 3 are transformed into (5.6) and (5.7), respectively.

The matrix multiplication involving Λ^k on the rhs of (5.6) and the vector addition involving $\mathcal{F}(T_k)$ in the 'numerator' on the rhs of (5.7) can be eliminated from these equations by the substitution of the 'solution' of (5.6) into the 'numerator' of (5.7) to yield

$$\mathcal{F}(T_k) + \widetilde{\Phi}^k = \mathcal{F}(T_k) + (I - \Lambda^k)^{-1} \Lambda^k \mathcal{F}(T_k) = (I - \Lambda^k)^{-1} \mathcal{F}(T_k). \tag{5.8}$$

Since, on the rhs of (5.8), we need the action of $(I - \Lambda^k)^{-1}$ on $\mathcal{F}(T_k)$, then it can be obtained by solving

$$(I - \Lambda^k) \Phi^k \equiv \mathcal{F}(T_k). \tag{5.9}$$

The above equation enable us to write (5.8) as $\mathcal{F}(T_k) + \widetilde{\Phi}^k = \Phi^k$, which when substituted into (5.7) yields

$$T_{k+1} = T_k + \frac{\Phi^k}{\frac{C_p^k + \dot{C}_p^k[T_k - T^n]}{\Delta t_n} + \sum_{g=1}^{n_{\hat{g}}} \sum_{d=1}^{n_{\hat{d}}} w_d (\sigma_g^k [\dot{B}_g^k] + \dot{\sigma}_g^k [B_g^k] - \dot{\sigma}_g^k [\psi_{g,d}^k])}. \tag{5.10}$$

Thus, the computation cost of the fourth and the sixth lines can be further lowered by transforming the pair (5.6) and (5.7) into the equivalent pair (5.9) and (5.10). The substitution of this pair of equations into Algorithm 3 leads to the algorithm derived by the Sherman–Morrison–Woodbury formula.

Algorithm 4 (A Sherman–Morrison–Woodbury algorithm for solving (2.4)).

$T_0 = T^n$
for $k = 0, 1, \ldots$
1. $H_{g,d}^k \psi_{g,d}^k = \sigma_g^k B_g^k + f_{g,d}^n$
2. $\mathcal{F}(T_k) = q - C_p^k \frac{T_k - T^n}{\Delta t_n} + \sum_{g=1}^{n_{\hat{g}}} \sum_{d=1}^{n_{\hat{d}}} \sigma_g^k w_d (\psi_{g,d}^k - B_g^k)$
3. if $\|\mathcal{F}(T_k)\| > tol$
4. $\quad (I - \Lambda^k) \Phi^k = \mathcal{F}(T_k)$
5. $\quad \lambda = 1$
6. $\quad T_\lambda = T_k + \lambda \frac{\Phi^k}{\frac{C_p^k + \dot{C}_p^k[T_k - T^n]}{\Delta t_n} + \sum_{g=1}^{n_{\hat{g}}} \sum_{d=1}^{n_{\hat{d}}} w_d (\sigma_g^k [\dot{B}_g^k] + \dot{\sigma}_g^k [B_g^k] - \dot{\sigma}_g^k [\psi_{g,d}^k])}$
7. $\quad$ if $\|\mathcal{F}(T_\lambda)\| > \|\mathcal{F}(T_k)\|$
8. $\quad\quad \lambda = \lambda/2$, go to 6
9. $\quad$ else
10. $\quad\quad T_{k+1} = T_\lambda$
11. $\quad$ end if
12. else
13. $\quad$ break, (solution found)
14. end if

end for.

Algorithm 4 is less expensive than Algorithm 3, since lines 4 and 6 of Algorithm 4 are less expensive than the corresponding lines of Algorithm 3. Let us compare lines 6 of these algorithms first. There are fewer operations in line 6 of Algorithm 4 than in line 6 of Algorithm 3. A big saving occurs in line 4; line 4 of Algorithm 4 requires the inversion of the $n_{\hat{x}} \times n_{\hat{x}}$ dense matrix $(I - \Lambda^k)$, but line 4 of Algorithm 3 requires the inversion of a $(n_{\hat{g}} \cdot n_{\hat{d}} \cdot n_{\hat{x}}) \times (n_{\hat{g}} \cdot n_{\hat{d}} \cdot n_{\hat{x}})$ transport matrix where the group-to-group coupling and the direction-to-direction coupling are described by an anisotropic 'fission matrix'.

Remark 7. If, in Algorithm 4, the matrix $(I - \Lambda^k)$ on the lhs of the fourth line and the matrix in 'denominator' of the fifth line are both nonsingular, then Algorithm 4 converges to the solution of (2.4) when $\mathcal{F}(T_k) = 0$.

Proof. When these two conditions are met, then Algorithm 4 can proceed. When $\mathcal{F}(T_k) = 0$, we have the solution to (2.4) for the reasons given in Remark 1. □

5.3. The solution of the Lambda equation

Algorithm 4 rests on the solvability of the lambda[7] equation on its fourth line; this equation is and shall be referred to as (5.9). Under a mild assumption, the matrix $I - \Lambda$ on the lhs of (5.9) is nonsingular.

Theorem 5.1. (*The matrix* $(I - \Lambda^*)$ *is nonsingular.*) *Assume that the Jacobian of* $\mathcal{F}$ *at* T^* *is nonsingular, where* T^* *is the solution of* $\mathcal{F}(T^*) = 0$, *then* $(I - \Lambda^*)$ *at* T^* *is nonsingular.*

Proof. This assumption on the Jacobian of a nonlinear system of equations is the condition required by Newton's method to solve the nonlinear system. Since the null space of **J** is empty, then the action of **J**, given by (8.3), on an arbitrary vector x is nonzero, i.e.

$$\left(\frac{C_p^* + \dot{C}_p^*[T^* - T^n]}{\Delta t_n} + \sum_{g=1}^{n_{\tilde{g}}} \sum_{d=1}^{n_{\hat{d}}} w_d (I - \sigma_g^* H_{g,d}^{*,-1})(\sigma_g^*[\dot{B}_g^*] + \dot{\sigma}_g^*[B_g^*] - \dot{\sigma}_g^*[\psi_{g,d}^*])\right) x \neq 0, \tag{5.11}$$

where the superscript* on a symbol means the symbol is evaluated at T^*.

Assuming that the nonzero vector y is a null vector of $(I - \Lambda^*)$, then

$$\Lambda^* y = y. \tag{5.12}$$

Let us rescale y by the nonsingular matrix of (4.23)

$$y = \left(\frac{C_p^* + \dot{C}_p^*[T^* - T^n]}{\Delta t_n} + \sum_{g=1}^{n_{\tilde{g}}} \sum_{d=1}^{n_{\hat{d}}} w_d (\sigma_g^*[\dot{B}_g^*] + \dot{\sigma}_g^*[B_g^*] - \dot{\sigma}_g^*[\psi_{g,d}^*])\right) z. \tag{5.13}$$

The substitution (5.5) and (5.13) into (5.12) yields

$$\left(\frac{C_p^* + \dot{C}_p^*[T^* - T^n]}{\Delta t_n} + \sum_{g=1}^{n_{\tilde{g}}} \sum_{d=1}^{n_{\hat{d}}} w_d (I - \sigma_g^* H_{g,d}^{*,-1})(\sigma_g^*[\dot{B}_g^*] + \dot{\sigma}_g^*[B_g^*] - \dot{\sigma}_g^*[\psi_{g,d}^*])\right) z = 0,$$

which contradicts (5.11). □

Since Λ^k is nonsymmetric (and $\|\Lambda^k\|$ may be larger than 1 when the coefficients are temperature dependent), then a Krylov method is needed to solve (5.9). In order to invert the matrix $(I - \Lambda^k)$ on the lhs of (5.9), a Krylov method requires a function that returns the action of $(I - \Lambda^k)$ on an arbitrary vector x. This function can be derived from (5.5) by multiplying both sides of the equation by x to yield

$$\Lambda^k x = \sum_{g=1}^{n_{\tilde{g}}} \sum_{d=1}^{n_{\hat{d}}} w_d \sigma_g^k H_{g,d}^{k,-1}(\alpha_{g,d}^k x),$$

where the term $H_{g,d}^{k,-1}\alpha_{g,d}^k x$ is determined by solving the equation $H_{g,d}^k \psi_{g,d}^k = \alpha_{g,d}^k x$.

5.4. Preconditioning the Lambda equation

The purpose of this section is to derive a preconditioner for $I - \Lambda^k$ by approximating Λ^k. Let us examine (5.5) in order to gain an understanding of Λ^k. If Λ^k were a diagonal matrix, then it would be easy to derive a

[7] Different kinds of lambda equations, derived by the application of SMW formula to transport equations, can be found in other applications of transport theory, e.g., the lower order equation of mono-energetic neutron transport, and the lambda equation of radiation line transport.

preconditioner for $I-\Lambda^k$. Since, according to (5.5), Λ^k is a linear combination of triple products $\sigma_g^k H_{g,d}^{k,-1}\alpha_{g,d}^k$, where σ_g^k and $\alpha_{g,d}^k$ are diagonal matrices and $H_{g,d}^{k,-1}$ is a dense matrix, then a preconditioner for $I-\Lambda^k$ can be derived by approximating $H_{g,d}^{k,-1}$ by a diagonal matrix. If we define $H_{g,d}^{k,\mathrm{diag}}$ to be the diagonal of $H_{g,d}^k$, then our approximation for $H_{g,d}^{k,-1}$ is

$$H_{g,d}^{k,-1} \approx (H_{g,d}^{k,\mathrm{diag}})^{-1}. \tag{5.14}$$

Substituting (5.14) into (5.5), we have a diagonal approximation for the lambda operator

$$\Lambda_{\mathrm{diag}}^k \equiv \sum_{g=1}^{n_{\tilde{g}}}\sum_{d=1}^{n_{\tilde{d}}} w_d \sigma_g^k (H_{g,d}^{k,\mathrm{diag}})^{-1}\alpha_{g,d}^k. \tag{5.15}$$

Let us examine $\Lambda_{\mathrm{diag}}^k$ and Λ^k for two limiting cases: vanishingly cross sections and infinite cross sections. As $\sigma_g^k \to 0$ under the constraint $\Delta t_n > 0$, both $\Lambda_{\mathrm{diag}}^k$ and Λ^k go to *0*. On the other hand, since $\|D\|/\|\sigma_g^k\| \to 0$ as $\|\sigma_g^k\| \to \infty$, then $H_{g,d}^k \to H_{g,d}^{k,\mathrm{diag}}$ as $\|\sigma_g^k\| \to \infty$. Hence $\Lambda_{\mathrm{diag}}^k$ and Λ^k agree in these two limits. The substitution of (5.15) into $(I-\Lambda^k)$ followed by inversion yields our preconditioner for (5.9)

$$P \equiv (I-\Lambda_{\mathrm{diag}}^k)^{-1}. \tag{5.16}$$

6. Numerical results

The algorithms presented in this paper are tested on three problems for efficiency and accuracy. The algorithms are the PFM of Algorithm 1, the semi-implicit nonlinear method (SiNL) of Algorithm 2, the isotropic nonlinear (INL) *approximation* of Algorithm 3 described in Section 5.1, and the SMW method of Algorithm 4. The nonlinear equations and the linear equations, which are solved by the algorithms, are summarized in Table 1. The table shows that the SiNL method solves $\mathcal{F}_{\mathrm{lag}}(T)=0$ but the other three solve $\mathcal{F}(T)=0$. Thus the SiNL solution is different from the solutions of the others. The magnitudes of the differences are illustrated in the plotted results.

The methods are preconditioned as follows. For the PFM method, we precondition **J** by the diagonal preconditioner of (5.15) rather than by the diffusion preconditioner derived in [11] in order to demonstrate the viability of the PFM method with simple preconditioning. The linear equation of the SiNL method is preconditioned by the GTA accelerator [20] which is preconditioned by the DSA accelerator [2,4,8,9,19,22]. In the linear equation of the INL algorithm, there are two types of 'α' coefficients; $\tilde{\alpha}_g^k$ of (5.2) is isotropic, but $\alpha_{g,d}^k$ of (4.25) is anisotropic. Since the operator on the lhs of the linear equation of the INL method is isotropic, this equation is preconditioned by GTA which is preconditioned by DSA. The linear equation of the SMW algorithm is solved by the GMRES [26] method preconditioned by the diagonal preconditioner of (5.15).

The algorithms derived in this paper are incomplete, because we assumed that the linear equations of the fourth lines of the algorithms, which determine the new iterate in Newton's method, are solved exactly. However, in practice, they are solved *inexactly* by iterative methods. Since our algorithms rely on line search to find the solution, and line searching requires an accurate direction in which to search, our algorithms may fail because this type of error is not accounted for by our line search; a failure of this type occurs in the third test problem of this paper. On the other hand, this type of error is less likely to cause a failure when it is properly accounted for in an Inexact Newton–Krylov solver such as Kinsol [12].

Although the PFM and SWM algorithms fit nicely into the framework of a Newton solver (because the linear equations and the nonlinear equations are in spaces of equal dimensions), the SiNL and INL algorithms

Table 1
The nonlinear equations and the linear equations solved by the Algorithms

Algorithm	Nonlinear equation	Linear equation
PFM	$\mathcal{F}(T)=0$	$\mathbf{J}\delta T = -\mathcal{F}(T_k)$
SiNL	$\mathcal{F}_{\mathrm{lag}}(T)=0$	$H_{g,d}\delta\psi_{g,d}^k - \hat{\alpha}_g^k \sum_{g'=1,d'=1}^{n_{\tilde{g}},n_{\tilde{d}}} \sigma_{g'} w_{d'} \delta\psi_{g',d'}^k = \hat{\alpha}_g^k \mathcal{F}_{\mathrm{lag}}(T_k)$
INL	$\mathcal{F}(T)=0$	$H_{g,d}^k\delta\psi_{g,d}^k - \tilde{\alpha}_g^k \sum_{g'=1,d'=1}^{n_{\tilde{g}},n_{\tilde{d}}} \sigma_{g'}^k w_{d'} \delta\psi_{g',d'}^k = \alpha_{g,d}^k \mathcal{F}(T_k)$
SMW	$\mathcal{F}(T)=0$	$(I-\Lambda^k)\Phi = \mathcal{F}(T_k)$

do not (because the linear equations of the SiNL and INL methods are in a higher dimensional space than the space of the nonlinear equations). Since the SiNL and the INL equations do not fit neatly into the framework of a Newton solver, we solved them with a home grown code which is written in a more general framework than the framework of a Newton solver. In order to compare the performances of the four algorithms within a common framework, the equations of the PFM and the SMW methods are also solved with our code. Solving them with our code does, however, a gross injustice to both, because our code is not built to handle a large search direction error. The results of the SMW obtained by Kinsol are given in Table 2 as a point of reference for the efficiency that could be achieved by the SMW method when it is linked to a well-tuned nonlinear solver such as Kinsol [12]. The PFM results obtained by Kinsol are not reported, since they are nearly identical to the SMW results obtained by Kinsol. In our code, the spatial derivative is discretized by the Simple Corner Balance method [1].

The three test problems, presented in the order of increasing temperature sensitivity, subject the approximations of the SiNL and INL methods to a sequence of increasingly stressful situations. Both $\dot{C}_p^k$ and $\dot{\sigma}_g^k$ are set to zero in the SiNL method, but only $\dot{\sigma}_g^k$ is set to zero in the INL method. Since the coefficients of the first test problem, which is from Larsen's work on Grey Transport Acceleration [20], are temperature insensitive, then the SiNL and INL methods are able to solve this problem accurately and efficiently. We shall say that the approximations of the SiNL and INL methods are 'unstressed' by Larsen's problem. The second test problem is from Su's and Olson's work [27] on an analytical solution of a radiation transport problem with a constant cross section and a temperature sensitive heat capacity which is proportional to T^3. The SiNL method solves this problem less accurately and less efficiently than the INL method. We shall say that the SiNL approximation is 'stressed' by Su's and Olson's problem, but the INL approximation is unstressed by it. The third test problem is an adaptation of the problem of Fleck and Cummings (FC) [14] in which the cross section of FC is modified to yield a temperature sensitive cross section. The solution to this problem is obtained with little accuracy and with difficulty by the INL method, but is obtained with even less accuracy

Table 2
Solver statistics for Problem 1

Δt	Method	Run time	Nonlinear	Back track	Linear
30	SiL	68	–	–	30
	PFM	1870	621	346	621
	SiNL	197	93	0	193
	INL	221	95	0	202
	SMW	512	73	0	73
	Kin-SMW	164	46	30	58
100	SiL	33	–	–	9
	PFM	738	232	174	230
	SiNL	91	55	6	73
	INL	100	53	6	76
	SMW	312	37	6	204
	Kin-SMW	116	38	9	74
300	SiL	16	–	–	3
	PFM	313	96	84	96
	SiNL	64	39	23	41
	INL	70	36	22	37
	SMW	338	31	16	239
	Kin-SMW	94	22	3	79
900	SiL	1	–	–	1
	PFM	154	45	49	45
	SiNL	72	35	53	35
	INL	74	29	45	29
	SMW	267	21	21	187
	Kin-SMW	107	16	1	117

and with even more difficulty by the SiNL method. We shall say that both methods are stressed by Fleck's and Cummings's problem.

6.1. Larsen's test problem

This test problem is from Larsen's paper on Grey Transport Acceleration [20]. We introduce this problem by beginning with a description of the problem's phase space grid. The frequency variable v is logarithmically spaced with 50 groups between $hv_{\min} = 10^{-5}$ keV and $hv_{\max} = 10$ keV. Group g is defined by $v_{g-\frac{1}{2}} \leqslant v \leqslant v_{g+\frac{1}{2}}$, where

$$v_{\frac{1}{2}} = v_{\min}, v_{g+\frac{1}{2}} = \left(\frac{v_{\max}}{v_{\min}}\right)^{\frac{1}{50}} v_{g-\frac{1}{2}}.$$

The angular quadrature is the 20 point Gauss–Legendre approximation; this set has five times more angles than the 4 point Gauss–Legendre set in Larsen's paper. The time steps are constant 30 ps (1 ps $= 10^{-12}$ s) increments. The spatial domain is divided into three regions which is described by the spatial mesh,

$$\Delta x = \begin{cases} .10 \text{ cm}, & 0 < x < 1, \\ .02 \text{ cm}, & 1 < x < 2, \\ .20 \text{ cm}, & 2 < x < 4. \end{cases}$$

We continue the introduction of Larsen's test problem with a description of the problem's physical parameters. The cross section models photo-ionization absorption which is corrected for stimulated emission

$$\sigma(v, T, x) = \gamma(x) \frac{1 - \mathrm{e}^{-hv/kT}}{(hv)^3}, \tag{6.1}$$

where

$$\gamma(x) = \begin{cases} 1 \text{ keV}^3/\text{cm}, & 0 < x < 1, \\ 1000 \text{ keV}^3/\text{cm}, & 1 < x < 2, \\ 1 \text{ keV}^3/\text{cm}, & 2 < x < 4. \end{cases} \tag{6.2}$$

We define $\sigma_g(T)$ to be the group average of the above formula at the zone centers;

$$\sigma_g(T) \equiv \frac{1}{v_{g+\frac{1}{2}} - v_{g-\frac{1}{2}}} \int_{v_{g-\frac{1}{2}}}^{v_{g+\frac{1}{2}}} \sigma(v, T, x_i) \mathrm{d}v.$$

The heat capacity C_p is the constant $5.109 \cdot 10^{14}$ erg keV^{-1} cm^{-3}.

We complete the introduction of Larsen's test problem with a description of the problem's energy sources. The initial temperature is $T(x, 0) = 10^{-3}$ keV, which is in equilibrium with the initial intensity $\psi_{g,d}(x, 0) = B_g(T(x, 0))$. No photons enters from the left boundary, but a steady, direction independent, 1 keV Planckian distribution of photons, $\psi_{g,d}(4 \text{ cm}, t) = B_g(1 \text{ keV})$, enters from the right boundary. The external heat source, q, and the external photon source, $s_{g,d}$, are both zero.

The coefficients of this problem is insensitive to temperature variations; the following lemma facilitates the proof of this statement.

Lemma 6.1. *The inequality* $xe^{-x} < (1 - e^{-x})$ *holds for* $x > 0$.

Proof. Since $\mathrm{e}^x = 1 + x + \frac{1}{2}x^2 + \cdots$, then $\mathrm{e}^x > 1 + x$, for $x > 0$. The substitution of this inequality into $\mathrm{e}^x\mathrm{e}^{-x} = 1$, yields $(1 + x)\mathrm{e}^{-x} < 1$, which upon rearrangement gives $x\mathrm{e}^{-x} < (1 - \mathrm{e}^{-x})$. □

By this lemma, $\sigma(v, T, x)$ of (5.1) is insensitive, because

$$\zeta(\sigma(v, T, x)) \equiv \left| \frac{T}{\sigma(v, T, x)} \frac{\partial \sigma(v, T, x)}{\partial T} \right| = \frac{hv}{kT} \frac{\mathrm{e}^{-hv/kT}}{1 - \mathrm{e}^{-hv/kT}} < 1, \quad \text{for } T \geqslant 0, \ v > 0.$$

Furthermore, the heat capacity is independent of temperature. Since the coefficients of this problem is insensitive to temperature, two results occur. First, the SiNL solution is expected to be accurate since $\mathcal{F}_{\text{lag}}(T)$ is an accurate approximation of $\mathcal{F}(T)$. Second, the SiNL and the INL estimates for T_λ are not only accurate but also can be solved efficiently by using the GTA method with DSA preconditioning. Therefore the SiNL and INL solve this problem accurately and efficiently. On the other hand, the PFM and SMW algorithms, which are built with simple preconditioners, require many GMRES iterations to determine T_λ.

Turning to mathematics, the theorem of [6] sets an upper bound and a lower bound for the temperature of this problem. The upper bound is the largest temperature amongst the temperatures by which the initial conditions and the boundary conditions of this problem are specified. These temperatures are the initial material temperature $T(x, 0) = 10^{-3}$ keV, the temperature of the Planckian distribution of the initial intensity $\psi_{g,d}(x, 0) = B_g(T(x, 0))$, the temperature of the Planckian distribution of photons on the right inflow boundary $\psi_{g,d}(4, t) = B_g(1\text{ keV})$, and the temperature of keV that characterizes the empty Planckian on the left inflow boundary. The lower bound of the theorem is the smallest of these temperatures. The temperature of this problem is therefore

$$0\text{ keV} \leqslant T(x,t) \leqslant 1\text{ keV}. \tag{6.3}$$

It was found in [11] that the SiL method yields solutions which lie outside of these limits when $\Delta t \geqslant 300$ ps, because the SiL method accepts a trial solution without testing the nonlinear residual of the trial solution. However, as we shall see, the SiNL and INL algorithms, built on top of a modification of the SiL equations, yield solutions which are within these limits.

Since the exact solution of this problem is not known analytically, we define the 'exact' solution to be the PFM solution, which is computed by Kinsol on the fine phase space grid which has 2 times more spatial zones and 30 times smaller time steps than the phase space grid described in the beginning of this section. The results at $t = 900$ ps for 4 different time steps are plotted in Fig. 1 and are tabulated in Table 2. For the two largest time steps, the SiL solution, which motivated this investigation, is outside of the limits of (6.3). On the other hand, the solutions of the nonlinear methods are within these limits. Furthermore, the solutions of the nonlinear methods are in close agreement with one other; a solution of $\mathcal{F}(T) = 0$ is in the proximity of the solution of $\mathcal{F}_{\text{lag}}(T) = 0$. The reason for the agreement is because the coefficients of this problem are insensitive to temperature variations; therefore $\mathcal{F}_{\text{lag}}(T)$ approximates $\mathcal{F}(T)$ well. Moreover, when the time step is increased, the solutions by the nonlinear methods depart from the 'exact' solution not randomly but in lock step, because the error is not due to not solving $\mathcal{F}(T) = 0$ but due to large Δt.

Table 2 shows the solver statistics for this problem. The statistics in last 4 columns of the table are: column 3 is the run time in seconds, column 4 is the total number of nonlinear iterations, column 5 is the total number of times that the back tracking parameter λ was reduced, column 6 is the total number of iterations which was needed to solve the linear equation. For each time step, we list 6 algorithms. The sixth, Kin-SMW, is the SMW method solved by Kinsol; it shows the efficiency of SMW method which could be attained by an optimized nonlinear solver. There are two reasons why SiNL and INL methods are faster than the PFM and SMW methods. The first is because the SiNL and INL methods are preconditioned by the GTA and DSA accelerators but the PFM and SMW are preconditioned by the crude preconditioner of (5.16). The second is because our home grown code 'over-solves' the linear equations to an accuracy which is not required by the nonlinear solver. The over-solving is revealed in the Kin-SMW and SMW statistics. The Kin-SMW statistics, which is the number of iterations needed by Kinsol, is smaller than the SMW statistics, which is the number of iterations needed by our code. Kinsol achieves efficiency by tuning its linear solver to its nonlinear solver.

We shall conclude the discussion of this problem by comparing the runtime/accuracy ratio of the SiL method to the runtime/accuracy ratio of the INL method which is our fastest nonlinear method for solving $\mathcal{F}(T) = 0$. The runtime/accuracy ratio of a method is difficult to determine, because we do not have the analytical solution to measure the accuracy of a numerical solution. However, the runtime/accuracy ratio of a method is, in some sense, related to the time to solution at the largest time step which can be taken by the method to yield a physical solution. Fig. 1 shows that the time step, which separates the physical solutions from the unphysical solutions, is between $\Delta t = 100$ ps and $\Delta t = 300$ ps for the SiL method; the solutions computed with a smaller time step are physical, but the solutions computed with a larger time step are unphysical. The run times of the SiL method for the time steps of 100 ps and 300 ps are 33 s and 16 s, respectively. However, the

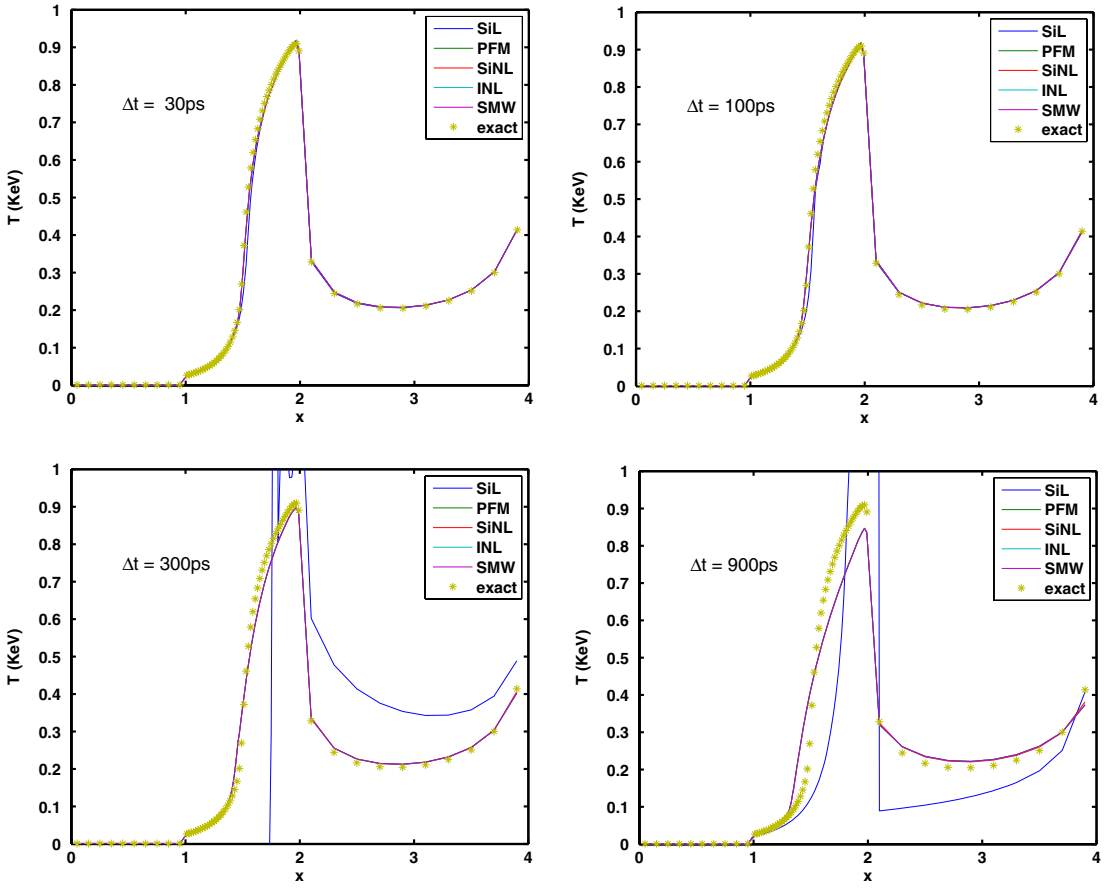

Fig. 1. Test runs for Problem 1 with 4 different time steps; $\Delta t = 30$, 100, 300, 900 ps. The SiL solutions, computed with $\Delta t = 300$ ps, and 600 ps, overshoot 1 keV and undershoot 0 keV.

INL method is able to compute a physical solution at the largest possible time step 900 ps for the time point $t = 900$ ps. In fact, the INL method is able to compute a physical solution at a much larger time step, but that solution would be beyond the time point 900 ps. The run time of the INL method for the time step of 900 ps is 74 s, which is an upper bound for the run time of the INL method for the largest time step by which it yields a physical solution. Therefore, our best guess for runtime/accuracy ratio of the INL method is <74, and our best guess for the runtime/accuracy ratio of the SiL method <33. These results show that the SiL method has the advantage of speed, but the INL method has the advantage of reliability (to deliver a physical solution).

6.2. The problem of Su and Olson

The problem of Su and Olson [27] puts great stress on the assumption that $\dot{C}_p^k$ is negligible, but puts no stress on the assumption that $\dot{\sigma}_g^k$ is small. The reason is: in the nonlinear system solved analytically by Su and Olson, $C_p(T)$ is temperature sensitive but $\sigma_g(T)$ is temperature independent. The system consists of the frequency integrated transport equation,

$$\left(\frac{1}{c}\frac{\partial}{\partial t} + \mu\frac{\partial}{\partial x} + \sigma\right) I(\mu, x, t) = \frac{1}{2}\sigma acT^4 + \frac{1}{2}acH\left(x - \frac{1}{2}\right)H\left(\frac{1}{2} - x\right)H\left(\frac{10}{c} - t\right),$$

and the material equation,

$$4aT^3\frac{\partial T}{\partial t} = \int_{-1}^{1} \sigma\left(I(\mu, x, t) - \frac{1}{2}acT^4\right)\mathrm{d}\mu,$$

where H is the Heaviside function, a is the radiation constant, c is the speed of light, and

$$I(\mu,x,t) \equiv \int_0^\infty \psi(v,\mu,x,t)\mathrm{d}v.$$

The initial conditions are $T(x,0) = 0$ and $I(\mu, x, 0) = 0$, and the boundary conditions are $\lim_{x\to\pm\infty} I(\mu, x, t) = 0$.

Since the sensitivity coefficient of the heat capacity $C_p(T) \equiv 4\ aT^3$ is

$$\zeta(C_p(T)) \equiv \left|\frac{T}{C_p(T)}\frac{\partial C_p(T)}{\partial T}\right| = 3,$$

then the SiNL assumption of setting $\dot{C}_p^k$ to 0 is tested by this problem. However, the cross section of this problem is constant; thus INL assumption of setting $\dot{\sigma}_g^k$ to zero (see (5.2)) is valid.

We simulate this problem as follows. The angular integral is approximated by the 20 point Gauss–Legendre quadrature. Since the problem is reflection symmetric, we solve the problem in the half space with the spatial grid,

$$\Delta x = \begin{cases} .020, & .0 < x < .1, \\ .100, & .1 < x < .5, \\ .125, & .5 < x < 1, \\ 1.00, & 1. < x < 35. \end{cases}$$

In the half space, no photons enters from the right boundary, and photons are reflected at the left boundary. The spatial derivative is approximated by the Simple Corner Balance method [1]. Since the algorithms cannot handle the singular perturbation caused by a vanishing heat capacity which occurs when the temperature is 0, we modify the initial temperature to be .001 everywhere.

In Fig. 2, there are 5 pairs of sub-figures which are ordered from left to right and from top to bottom. Each pair of sub-figures represent the results by a method: sub-figures 1 and 2 are the pair of results for the SiL method, sub-figures 3 and 4 are the pair of results for the PFM method, sub-figures 5 and 6 are the pair of results for SiNL method, sub-figures 7 and 8 are the pair of results for the INL method, and sub-figures 9 and 10 are the pair of results for the SMW method. The first sub-figure of a pair contains the plots of the spatial profiles of the fourth power of the material temperature at three time points, and the second sub-figure of the pair contains the plots of the spatial profiles of the photon energy at the same time points. The profiles were calculated with a constant time step of .1/20, the largest time step with which we found reasonable agreement with the analytical solution. However, the SiL method needs a time step of .1/2000 to achieve a solution of comparable accuracy. Furthermore, DSA was turned off in the SiL calculation since the effective absorption by the small time step rendered the SiL equation nondiffusive. The results of the PFM, the INL, and the SMW algorithms agree with the analytical solution of Su and Olson, but the results of the SiNL algorithm, as expected, do not. Furthermore, Table 3 shows that the solver statistics of the PFM, INL, and SMW algorithms are similar.

We shall conclude our presentation of the problem of Su and Olson by comparing the runtime/accuracy ratio of the SiL method to the runtime/accuracy ratio of the INL method. Since the SiL and INL solutions of Fig. 2 are of comparable accuracy for this problem, we can read off these ratios from the runtime column of Table 3. They are 4508 s for the SiL method and 50 s for the INL method. These run times represent runtime/accuracy ratios of the methods more accurately than the run times of Larsen's problem, because the accuracy of a numerical solution can be measured by the analytical solution of Su and Olson. For this problem, we can say with a degree of certainty that the INL method is more than 10 times faster than the SiL method (see Table 4).

6.3. The problem of Fleck and Cummings

Fleck and Cummings (FC) [14] examined two types of cross sections; the first type depends weakly on the temperature, but the second type depends strongly on the temperature. The first type, $27\ (1 - \mathrm{e}^{-h\nu/kT})(h\nu)^{-3}$, is

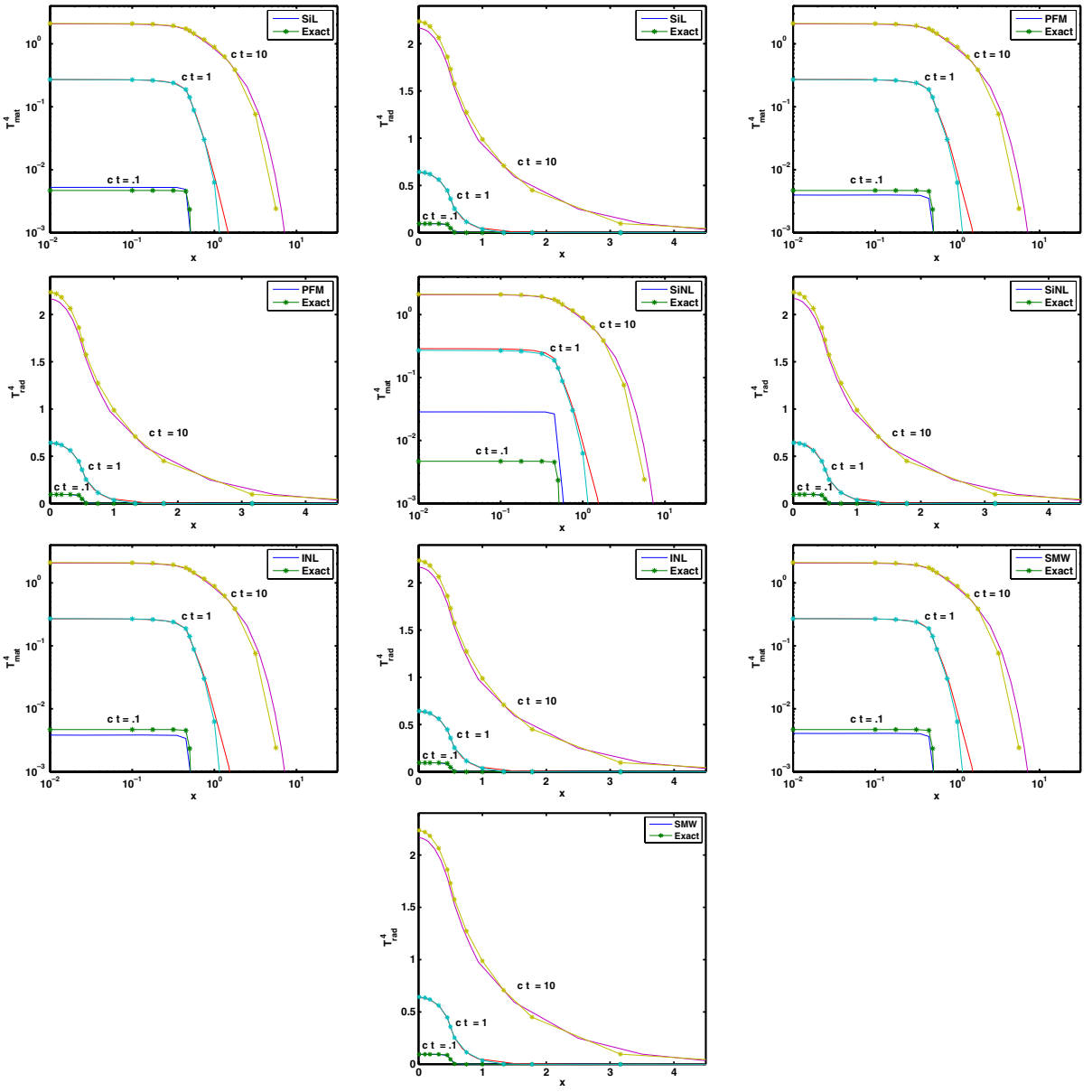

Fig. 2. The fourth power of the material temperature is on the left, and radiation energy density is on the right.

Table 3
Solver statistics for the calculations graphed in Fig. 2

	Run time	Nonlinear	Back track	Linear
SiL	4508	–	–	40,000
PFM	41	416	40	417
SiNL	46	405	30	810
INL	50	420	43	423
SMW	42	423	35	423
Kin-SMW	24	440	400	440

Table 4
Solver statistics for Problem 3

Δt	Method	Run time	Nonlinear	Back track	Linear
10	SiL	22	–	–	30
	PFM	267	87	11	87
	SiNL	96	43	0	43
	INL	180	103	0	103
	SMW	386	35	0	224
30	SiL	8	–	–	10
	PFM	148	48	21	48
	SiNL	32	14	1	14
	INL	134	89	4	89
	SMW	206	19	0	99
60	SiL	4	–	–	5
	PFM	89	29	16	29
	SiNL	21	12	0	12
	INL	78	46	16	46
	SMW	151	14	1	61
300	Kin-SMW	147	26	1	169

essentially the insensitive cross section (6.1) used by Larsen to test the SiL method [20]. The cross section of the second type

$$\sigma(v,T,x) = 27\frac{1-\mathrm{e}^{-hv/kT}}{(hv)^3 T^{\frac{3}{2}}}. \tag{6.4}$$

is the cross section of the first type divided by $T^{\frac{3}{2}}$. Even though (6.4) is unbounded for $T = 0$, its sensitivity as measured by (5.1) is not larger than *1* for all T. Thus, the question of whether the SiNL and INL methods can take large time steps when solving a problem with a temperature sensitive cross section is not answered by (6.4). In order to turn (6.4) into a temperature sensitive cross section, we replace the stimulated emission factor $(1-\mathrm{e}^{-hv/kT})$ with the number 1. We also generalize the cross section slightly by replacing the number 27 with the $\gamma(x)$ function of (6.2) to model a spatial variation. These two modifications yield the cross section

$$\sigma(v,T,x) = \frac{\gamma(x)}{(hv)^3 T^{\frac{3}{2}}}, \tag{6.5}$$

with the sensitivity coefficient $\zeta(\sigma(v,T,x)) = \frac{3}{2}$. Since $\dot{\sigma}_g^k$ is significant, this problem tests not only the lagging assumption of the SiNL approximation but also the isotropicization assumption of the INL approximation.

However, the infinity of (6.5) at $T = 0$ interferes with our examination of these approximations. The interference consists of third factors. The first factor is that the transport equation with (6.5) as the cross section is outside of the scope of the theorem derived by [6]. Without this kind of theorem, we can not verify that a numerical solution is within the mathematical limits of the solution to the continuous transport equation. The second factor is that the infinity is not stabilized by implicit time differencing. The third factor, which is related to the second factor, is that the discretization error (proportional to $\mathrm{d}\sigma_g/\mathrm{dT}$) in the neighborhood of $T = 0$ is enormous. In order to compensate for the magnitude of this factor, Δt must be small. Therefore, the time step which is needed to yield a physical solution is limited not by the method to solve a system of algebraic equations, but by the discretization of the continuous equation which is a more fundamental aspect of the computational problem. We shall find that the time steps needed by the method presented in this paper to solve Fleck's and Cummings's problem are much smaller than the time steps needed by them to solve Larsen's problem.

The third test problem is a modification of the first problem; the cross section of (6.1) is replaced by the cross section of (6.5). Except for this difference, the problems are constructed from common building blocks: boundary conditions, initial conditions, and phase space mesh. Since this problem is more sensitive to temper-

ature variations than the first problem, our home grown code solves this problem with more difficulty than the first problem. Our code stalls on all 4 methods when $\Delta t = 100$ ps; the time step in which time discretization error is discernible.

The results at $t = 300$ ps, calculated by the three different time steps {10, 30, 60} ps, are displayed in Fig. 3. The 'exact' solution is obtained by the PFM method solved by Kinsol on a spatial grid with twice as many zones and with the time step of 1 ps. The results show that the lagging assumption of the SiNL approximation is inappropriate for this problem when the time step is 60 ps or larger. The results also show that the solutions of the PFM, INL, and SMW methods agree with the 'exact' solution for these time steps. However, our implementations of the 4 algorithms fail to converge when the time step is increased to 100 ps. On the other hand, Kinsol converges for a time step of 300 ps.

This failure by our code exposes the fragility of line searching when it is tied to an *inexact* Newton method. Line searching requires an accurate direction in which to search, but the direction, which is determined by the linear equation in Newton's method, is given approximately by an iterative solver. There is no reason to expect a line search to succeed when the linear equation, which is the transport equation of Algorithm 3, is approximated by isotropicization, nor is there a reason to expect it to succeed if the solution to the linear equation is returned inaccurately by an iterative solver.

The resolution of this difficulty is algorithm specific. Eisenstadt and Walker (EW) [13] show how line searching can be tied to a Krylov solver in the Inexact Newton–Krylov method. However, neither the INL method nor the SMW method are conventional Newton methods; the linear equation of the INL method is in a higher dimensional space than nonlinear equation, the linear equation of SMW is not the Jacobian of the nonlinear equation. Since the SMW method can be handled by Kinsol, we tried to incorporate the ideas

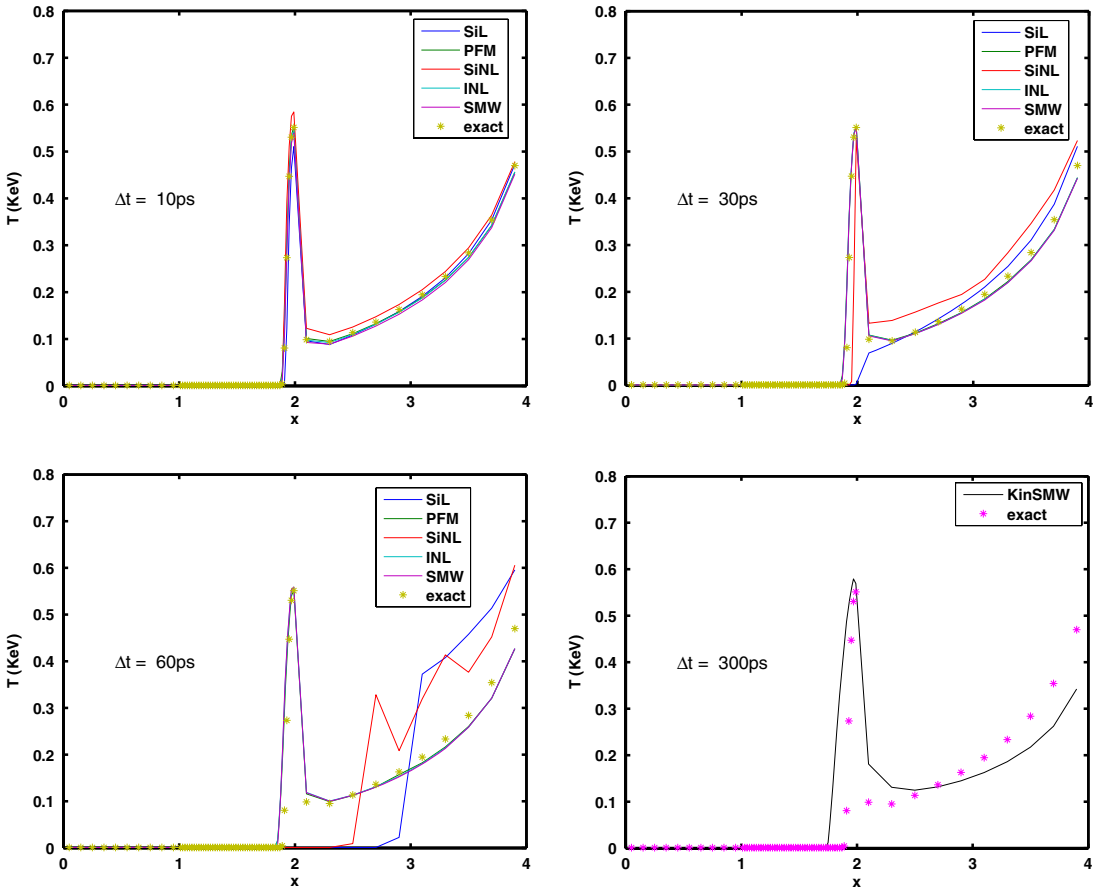

Fig. 3. Test runs for Problems 3 with 4 different time steps; $\Delta t = 10, 30, 60, 300$ ps.

of EW into our code. However, the difference in the statistics of the SMW method and statistics of the Kin-SMW method suggests that the EW method is not implemented in our code in the way that it is intended. On the other hand, we made no attempt to tie line searching to the GTA method, since the EW method which is derived for an inexact Newton solver is not applicable to this situation.

We shall conclude our presentation of the FC problem by examining the run times of the SiL and INL methods which are determined at the largest time steps which can be taken by them to yield physical solutions. This time step is larger than 10 ps for the SiL method, and is larger than 60 ps for the INL method. The run times are smaller than 22 s and smaller than 78 s for the SiL and INL methods, respectively. Hence, our best guess for the runtime/accuracy ratio for the SiL method is smaller than 22 s, our best guess for the runtime/accuracy ratio of the INL method is smaller than 78 s. Thus, the runtime/accuracy ratio of the INL method is almost 4 times larger than the runtime/accuracy ratio of the SiL method. However, these run times represent the runtime/accuracy of these methods less accurately than the run times of Larsen's problems, because these run times are interfered with by the infinity at $T = 0$.

7. Discussion

In this paper, we derive a modified SiL transport Eq. (4.24) to determine the next iterate in Newton's method to solve the radiation Eq. (3.3) derived by the PFM method. The pair of Eqs. (3.3) and (4.24) can be solved by either the INL method or the SMW method. Since, in addition to these two methods, the solution to (3.3) can be obtained by the PFM method, then one may ask: Which of the three, INL or SMW or PFM, is the best method? However, in order to narrow down the scope of this question, we shall first show in Section 7.1 that the PFM and SMW methods are equivalent. Then, in Section 7.2, we shall answer the question with the answer to the narrower question: Which of the pair, INL or SMW, is the better method? The SiL and SiNL methods shall also be assessed in the context of this pair in Section 7.2.

7.1. The PFM method of Algorithm 1 is equivalent to the SMW method of Algorithm 4

Except for the equations on lines 4 and 6 of Algorithm 1 and the equations on lines 4 and 6 of Algorithm 4, the equations on the other lines of the algorithms are identical. These seemingly unrelated pairs of equations are, however, related by a simple change of variable which connects δT of Algorithm 1 to Φ^k of Algorithm 4. The goal of this subsection is to uncover the relationship between these variables.

Let the diagonal matrix on the lhs of (4.23) be defined as

$$\Gamma^k \equiv \frac{C_p^k + \dot{C}_p^k[T_k - T^n]}{\Delta t_n} + \sum_{g=1}^{n_{\hat{g}}} \sum_{d=1}^{n_{\hat{d}}} w_d(\sigma_g^k[\dot{B}_g^k] + \dot{\sigma}_g^k[B_g^k] - \dot{\sigma}_g^k[\psi_{g,d}^k]) \tag{7.1}$$

to facilitate our investigation. Moreover, Γ^k is the 'denominator' on the rhs of line 5 of Algorithm 4, and is also the 'denominator' on the rhs of (4.25).

Lemma 7.1. *The negative of the product of* $(I - \Lambda^k)$ *and* Γ^k *is the Jacobian* $\partial\mathcal{F}/\partial T$, *that is*

$$-(I - \Lambda^k)\Gamma^k = \left.\frac{\partial \mathcal{F}(T)}{\partial T}\right|_{T_k},$$

where $\partial\mathcal{F}/\partial T$ *is given by (8.3) of Appendix.*

Proof. Writing $\alpha_{g,d}^k$ of (4.25) in terms of Γ^k defined in (7.1), we have

$$\alpha_{g,d}^k \equiv \frac{\sigma_g^k[\dot{B}_g^k] + \dot{\sigma}_g^k[B_g^k] - \dot{\sigma}_g^k[\psi_{g,d}^k]}{\frac{C_p^k + \dot{C}_p^k[T_k - T^n]}{\Delta t_n} + \sum_{g=1}^{n_{\hat{g}}} \sum_{d=1}^{n_{\hat{d}}} w_d(\sigma_g^k[\dot{B}_g^k] + \dot{\sigma}_g^k[B_g^k] - \dot{\sigma}_g^k[\psi_{g,d}^k])} = (\sigma_g^k[\dot{B}_g^k] + \dot{\sigma}_g^k[B_g^k] - \dot{\sigma}_g^k[\psi_{g,d}^k])(\Gamma^k)^{-1}. \tag{7.2}$$

The right multiplication of both sides of (5.5) by Γ^k followed by the substitution of (7.2) into the rhs of (5.5) yields

$$\Lambda^k \Gamma^k = \sum_{g=1}^{n_{\tilde{g}}} \sum_{d=1}^{n_{\tilde{d}}} w_d \sigma_g^k H_{g,d}^{k,-1} (\sigma_g^k [\dot{B}_g^k] + \dot{\sigma}_g^k [B_g^k] - \dot{\sigma}_g^k [\psi_{g,d}^k]). \tag{7.3}$$

The subtraction of (7.3) from (7.1) yields

$$(I - \Lambda^k)\Gamma^k = \frac{C_p^k + \dot{C}_p^k [T_k - T^n]}{\Delta t_n} + \sum_{g=1}^{n_{\tilde{g}}} \sum_{d=1}^{n_{\tilde{d}}} w_d (I - \sigma_g^k H_{g,d}^{k,-1})(\sigma_g^k [\dot{B}_g^k] + \dot{\sigma}_g^k [B_g^k - \psi_{g,d}^k]). \tag{7.4}$$

However, by (8.3), the rhs of (7.4) is equal to $-\frac{\partial \mathcal{F}(T)}{\partial T}|_{T_k}$, which proves the theorem. □

Lemma 7.2. *The fourth lines of Algorithms 4 and 1 are equivalent.*

Proof. The fourth line of Algorithm 4 is

$$(I - \Lambda^k)\Phi^k = \mathcal{F}(T_k).$$

Inserting $\Gamma^k (\Gamma^k)^{-1}$ between $(I - \Lambda^k)$ and Φ^k, and substituting (7.4) into the result give

$$\left.\frac{\partial \mathcal{F}(T)}{\partial T}\right|_{T_k} (\Gamma^k)^{-1} \Phi^k = -\mathcal{F}(T_k), \tag{7.5}$$

which is equivalent to the equation on the fourth line of Algorithm 1. □

Lemma 7.3. *Algorithms 4 and 1 are related by the change of variables*

$$\Phi^k = \Gamma^k \delta T. \tag{7.6}$$

Proof. Since the fourth line of Algorithm 4 can be written as (7.5), then the substitution of (7.6) into this equation gives the fourth line of Algorithm 1. Furthermore, the substitution of (7.6) into the rhs of the sixth line of (4) gives the sixth line of Algorithm 1. □

7.2. Conclusion

In this paper, a modified SiL transport Eq. (4.24) is derived to determine the next iterate in Newton's method to solve the PFM system of nonlinear equations (3.3). The INL and SMW methods, which unite the SiL method to the PFM method, can take time steps which are considerably larger than the time step that can be taken by the SiL method, and yield physical solutions when the SiL method yields an unphysical solution. Although the INL and SMW solve the modified SiL transport equation (4.24) by different approaches, they yield numerically equivalent solutions because they both solve the PFM system of nonlinear equations (3.3). The question on the superiority of the two will be decided by their preconditioners. The preconditioning of the SMW method is at the stage of a work in progress. On the other hand, the INL method is amenable to GTA and DSA preconditioning. Therefore, at the writing of this paper, the INL method is the better of the two, because its preconditioners, GTA and DSA, are superior to the preconditioners of the SMW method (and the closely related PFM method).

The reason why the SiL method yields an unphysical solution can be understood by studying the effects caused by the removal of terms from (3.2) and (4.24) to retrieve the SiL transport equation. Lagging the heat capacities and the cross sections of these equations takes us halfway to the SiL method; it removes terms from these equations to yield the SiNL method which is a slight modification of the SiL method. However, the removal of terms from (3.2) by the lagging of its coefficients produces a discernible error in the SiNL solution of the Su and Olson problem, and in the SiNL solution of the Fleck and Cummings problem. On the other hand, if the heat capacity and the cross section are temperature independent, no error is introduced into the SiNL solution, because the INL method simplifies to the SiNL method. Although the SiNL method is a slight modification of the SiL method, Larsen's test problem shows that the modification enables the SiNL method to yield physical solutions in situations when the SiL method can not. Going from the SiNL method

to the SiL method requires three additional steps: the temperature T_k in (4.7) and (4.8) is fixed to T^n, (4.8) is substituted into (4.7), and (4.5) is used to simplify the result to yield (2.23) of [20] which is (4.3) with T_k set to T^n. However, fixing T_k to T^n in $\mathcal{F}_{\text{lag}}(T_k)$ of (4.8) produces an error which is more deleterious than the lagging approximation error by preventing the temperature from attaining its physical state T^*. The result is an unphysical solution.

Acknowledgement

This work was performed under the auspices of the US Department of Energy by Lawrence Livermore National Laboratory under Contract No. W-7405-Eng-48. UCRL-JRNL-222808.

Appendix. The Jacobian of the photon free method

The goal of this appendix is to derive a formula for the Jacobian of $\mathcal{F}(T)$ by the differentiation of (3.2) with respect to T. Differentiating (3.2) with respect to T yields

$$\left.\frac{\partial \mathcal{F}(T)}{\partial T}\right|_{T_k} = -\frac{C_p^k + \dot{C}_p^k[T_k - T^n]}{\Delta t_n} - \sum_{g=1}^{n_{\tilde{g}}}\sum_{d=1}^{n_{\tilde{d}}} w_d(\dot{\sigma}_g^k[B_g^k - \psi_{g,d}^k] + \sigma_g^k[\dot{B}_g^k - \dot{\psi}_{g,d}^k]). \tag{8.1}$$

On the other hand, the differentiation of the first equation of (2.4) by T yields

$$H_{g,d}^k \dot{\psi}_{g,d}^k + \dot{\sigma}_g^k \psi_{g,d}^k = \sigma_g^k \dot{B}_g^k + \dot{\sigma}_g^k B_g^k. \tag{8.2}$$

If we solve (8.2) for $\dot{\psi}_{g,d}^k$, substitute the solution into (8.1), and rearrange the result slightly, then we have

$$\left.\frac{\partial \mathcal{F}(T)}{\partial T}\right|_{T_k} = -\frac{C_p^k + \dot{C}_p^k[T_k - T^n]}{\Delta t_n} - \sum_{g=1}^{n_{\tilde{g}}}\sum_{d=1}^{n_{\tilde{d}}} w_d(I - \sigma_g^k H_{g,d}^{k,-1})\left(\sigma_g^k[\dot{B}_g^k] + \dot{\sigma}_g^k[B_g^k - \psi_{g,d}^k]\right). \tag{8.3}$$

References

[1] M.L. Adams, Sub-cell balance methods for radiative transfer on arbitrary grids, Transp. Theory Stat. Phys. 26 (1997) 385–431.
[2] M.L. Adams, E.W. Larsen, Fast iterative methods for discrete-ordinates particle transport calculations, Prog. Nucl. Energ. 40 (1) (2002) 3–159.
[3] M.L. Adams, P. Nowak, Asymptotic analysis of a computational method for time = and frequency-dependent radiation transfer, J. Comp. Phys. 146 (1998) 366–403.
[4] R.E. Alcouffe, Diffusion synthetic acceleration methods for the diamond-difference discrete-ordinates equations, Nucl. Sci. Eng. 64 (1977) 344–355.
[5] L. Armijo, Minimization of functions having Lipschitz-continuous first partial derivatives, Pacific J. Math. 16 (1966) 1–3.
[6] E.S. Amdreev, M. Yu. Kozmanov, E.B. Rachilov, The maximum principle for a system of equations of energy and non-stationary radiation transfer, USSR Comput. Maths. Math. Phys. 23 (1) (1983) 104–109.
[7] Y.Y. Azmy, The weighted diamond-difference form of nodal transport methods, Nucl. Sci. Eng. 98 (1988) 29–40.
[8] B. Bihari, P.N. Brown, A linear algebraic analysis of diffusion synthetic acceleration for the boltzmann transport equation II: the simple corner balance method. Preprint.
[9] P.N. Brown, A linear algebraic development of diffusion synthetic acceleration for three-dimensional transport equations, Siam J. Numer. Anal. 32 (1) (1995) 179–214.
[10] B.G. Carlson, K.D. Lathrop, Transport theory the method of discrete ordinates, in: H. Greenspan, C.N. Kelber, D. Okrent (Eds.), Computing Methods in Reactor Physics, Gordon and Breach, New York, 1968, pp. 167–266.
[11] B. Chang, A deterministic photon free method to solve radiation transfer equations, J. Comp. Phys 222 (2007) 71–85.
[12] A.M. Collier, A.C. Hindmarsh, R. Serban, C.S. Woodward, User Documentation for KINSOL v2.3.0, Lawrence Livermore National Lab, UCRL-SM-208116.
[13] S.C. Eisenstadt, H.F. Walker, Choosing the forcing terms in an inexact Newton method, SIAM J. Sci. Comput. 17 (1996) 16–32.
[14] J.A. Fleck Jr., J.D. Cummings, An implicit Monte Carlo scheme for calculating time and frequency dependent nonlinear radiation transport, J. Comp. Phys. 8 (1971) 315–342.
[15] G.H. Golub, C.F. Van Loan, Matrix Computations, John Hopkins, Baltimore, 1991.
[16] A. Greenbaum, J.M. Ferguson, A Petrov–Galerkin finite element for solving the neutron transport equation, J. Comp. Phys. 64 (1986) 97–111.

[17] I. Hubeny, Accelerated Lambda Iteration: An Overview, Stellar Atmosphere Modeling, in: I. Hubeny, D. Mihalas, K. Werner (Eds.), Proceedings of an International Workshop, Tubingen, 8–12 April 2002, The Astronomical Society of the Pacific, San Fran.
[18] C.T. Kelley, Iterative methods for linear and nonlinear equations, Frontiers in Applied Mathematics, SIAM, 1995.
[19] E.W. Larsen, Unconditionally stable diffusion-synthetic acceleration methods for the slab geometry discrete ordinates equations. Part I: theory, Nucl. Sci. Eng. 82 (1982) 47–63.
[20] E.W. Larsen, A grey transport acceleration method for time-dependent radiative transfer problems, J. Comp. Phys. 78 (2) (1988) 459–480.
[21] E.W. Larsen, B. Mercier, Analysis of a Monte Carlo method for nonlinear radiative transfer, J. Comp. Phys. 71 (1987) 50–64.
[22] D.R. McCoy, E.W. Larsen, Unconditionally stable diffusion-synthetic acceleration methods for the slab geometry discrete ordinates equations. Part II: numerical results, Nucl. Sci. Eng. 82 (1982) 47–63.
[23] J.E. Morel, T.A. Wareing, K. Smith, A linear-discontinuous spatial difference scheme for S_n radiative transfer calculations, J. Comp. Phys. 128 (1996) 445–462.
[24] P.F. Nowak, M. Nemanic, Radiation Transport Calculations on Unstructured Grids using a Spatial Decomposed and Threaded Algorithm, Lawrence Livermore National Lab, UCRL-JC-133787.
[25] W.H. Reed, T.R. Hill, Triangular Mesh Methods for the Neutron Transport Equation, LA-UR-73-479, Los Alamos National Laboratory, 1973.
[26] Y. Saad, Iterative Methods for Sparse Linear Systems, PWS Publ. Co., Boston, 1996.
[27] B.J. Su, G.L. Olson, An analytic benchmark for nonequilibrium radiative transfer in an isotropically scattering medium, Ann. Nucl. Energy 24 (13) (1977) 1035–1055.